BULETINUL INSTITUTULUI POLITEHNIC DIN IAŞI

Tomul LVII (LXI)

Fasc. 1

ŞTIINȚA ŞI INGINERIA MATERIALELOR

2011 **Editura POLITEHNIUM**

BULETINUL INSTITUTULUI POLITEHNIC DIN IAŞI
PUBLISHED BY
„GHEORGHE ASACHI" TECHNICAL UNIVERSITY OF IAŞI
Editorial Office: Bd. D. Mangeron 63, 700050, Iaşi, ROMÂNIA
Tel. 40-232-278683; Fax: 40-232-237666; e-mail: polytech@mail.tuiasi.ro

Editorial Board

Editorial Advisory Board

BULETINUL INSTITUTULUI POLITEHNIC DIN IAŞI
BULLETIN OF THE POLYTECHNIC INSTITUTE OF IAŞI
Tomul LVII (LXI), Fasc. 1 2011

ŞTIINȚA ŞI INGINERIA MATERIALELOR

SUMAR

BULETINUL INSTITUTULUI POLITEHNIC DIN IAŞI
BULLETIN OF THE POLYTECHNIC INSTITUTE OF IAŞI
Tomul LVII (LXI), Fasc. 1 2011

MATERIALS SCIENCE AND ENGINEERING

CONTENTS

BULETINUL INSTITUTULUI POLITEHNIC DIN IAŞI
Publicat de
Universitatea Tehnică „Gheorghe Asachi” din Iaşi
Tomul LVII (LXI), Fasc. 1, 2011
Secția
ŞTIINȚA ŞI INGINERIA MATERIALELOR

CHEMICAL PROCEDURES FOR METALLIC SURFACE PREPARATION FOR THIN COATINGS DEPOSITION PROCESS (I)

BY

RAMONA HANU CIMPOEŞU[1*], CONSTANTIN BACIU[1], MARICEL AGOP[2], GABRIEL DUMITRU PĂDURARU[3], NICANOR CIMPOEŞU[1] and VASILE MANOLE[1]

"Gheorghe Asachi" Technical University of Iaşi,
[1]Faculty of Materials Science and Engineering
[2]Department of Physics
[3]Chemical Engineering and Environmental Protection Faculty

Received: February 14, 2011
Accepted for publication: March 28, 2011

Abstract. Thin coatings deposition on metallic substrates is an improvement method of materials, especially those used in the medical field as in contact body applications. Few chemical engraving methods including anodizing were used to prepare the shape memory alloy wire surface for further thin metallic or non metallic films deposition. Chemical, by EDAX, and microstructure, with SEM, analyses are made to establish some surface characteristics after the surface modification processes.

Key words: coatings deposition, metallic surface, shape memory alloy.

1. Introduction

Surface modification and coating of Nitinol (an acronym for NiTi Naval Ordnance Laboratory), a family of nearly equiatomic NiTi alloys with shape memory and superelastic properties, is a subject of numerous recent studies directed

*Corresponding author; *e-mail*: ramonahanu@yahoo.com

at improving the material's corrosion resistance as well as its biocompatibility through elimination of Ni from the surface. This chemical element is known to be allergenic and toxic, though essential for the human body. Although it has been shown that the amount of Ni recovered in biological studies in vitro may be either very low from the beginning or drop to undetectable levels after a brief exposure to biological environments (Wever *et al*., 1998; Cui *et al*., 2005) 'the nickel case' keeps reappearing. Thus, the recent results obtained on commercial ready-to-use orthodontic wires showed that the Ni release varied in a wide range from 0.2 to 7l g cm^2 (Arndt *et al.,* 2005). Moreover, it has been reported that the Ni release can actually significantly increase with time (Sui *et al*., 2006; Kobayashi *et al*., 2005; Bogdanski *et al*., 2005; Clarke *et al*., 2006), maintaining a high level up to 8 weeks and even for a few months (Bogdanski *et al*., 2005; Clarke *et al*., 2006), indicating the need for better understanding of the material/surface interface.

Based on the number of published papers on Nitinol surfaces, especially recently, one might conclude that this issue indeed deserves serious attention. Various techniques and protocols have been used for surface treatments; among them mechanical and electrochemical treatments, chemical etching, heat treatments, conventional and plasma ion immersion implantation, laser and electron-beam irradiation, design of bioactive surfaces, and a proper technique can easily be lost in that jungle of publications. Some of the procedures that were developed originally for pure Ti and their application to NiTi not only may not bring any improvement but, rather, can cause surface damage because of inevitable Ni involvement.

The electrochemistry of Nitinol is poorly explored. Until recently, there have been no studies on electro-polishing and anodizing of this material. This situation is gradually improving with the publications of papers on electro-polishing processes in various electrolytes (Pohl *et al*., 2004), and anodizing in various solutions and voltage regimes (Shi *et al*., 2007). The effect of chemical etching (passivation) in $HF+HNO_3$ aqueous solutions on Nitinol surface chemistry has also been studied (Shabalovskaya *et al*., 2003).

In this study few chemical surface modification methods are analyzed to improve the adhesion on Nitinol with further superficial thin layers that can be deposited on them.

2. Experimental Details

A superelastic echiatomic NiTi shape memory alloy (www.saesgetters.com) acquisitioned from Saes Getters Group was prepared through different engraving solution for thin layers deposition operation. The shape memory alloy has 50.5% Ni and 49.5% Ti mass percentages and an oxide layer on the wire surface. The material was "attack" with different solutions like 34% H_2SO_4 + 12% HCl, 48% H_2SO_4 + 18 % HCl and anodization processes. Microstructure of alloy surface before and after chemical treatments were analyzed using SEM

equipment with a SE detector and 30 KV alimentation tension of the gun lamp. Using an EDAX equipment chemical analysis were performed on 2.5 mm^2 surfaces following especially the Ni and Ti percentage evolution and also the other elements from the surface like oxygen, fluorine, sodium or carbon.

3. Experimental Results

Various techniques and protocols to have been used for surface treatments; among them mechanical and electrochemical treatments, chemical etching, heat treatments, conventional and plasma ion immersion implantation, laser and electron-beam irradiation, design of bioactive surfaces, and a proper technique can easily be lost in that jungle of publications. Some of the procedures that were developed originally for pure Ti and their application to NiTi not only may not bring any improvement but, rather, can cause surface damage because of inevitable Ni involvement.

The surface state of shape memory alloy NiTi is presented in Fig. 1 at a 250x power amplification of the image and a 50 μm scale. Can be observing a smooth surface of the material obtained from the element manufacturing that had a preparation necessity for better adhesion of the superficial layers ready for deposition.

Fig. 1 – SEM microscopy of NiTi surface as takenat a 250x power amplification.

In a first stage, the material was treated with a 34% H_2SO_4 + 12% HCl solution for 60 minutes at room temperature and the effects are presented in Fig. 2 in two characteristic microscopies at 300x and 1000x amplification power. The results present an affected surface on entire area with many holes in materials, made especially from lose of titan and nickel oxides, no larger than 2-5 μm.

The electrolytic etching explored in this case induced highly porous NiTi surfaces that might lead to enhanced Ni release. In Table 1 is presented the chemical composition of the shape memory surface after the chemical process applied. Both nickel and titanium elements decrease comparing with the initial composition most of these percentages lost are based on oxides form like TiO and the appearance of a chloride element on the material surface. Increasing the solution concentration to 48% H_2SO_4+18 % HCl and maintaining a similar exposure time the results are\presented in Fig. 3 as microstructures and Table 2 as chemical composition variation.

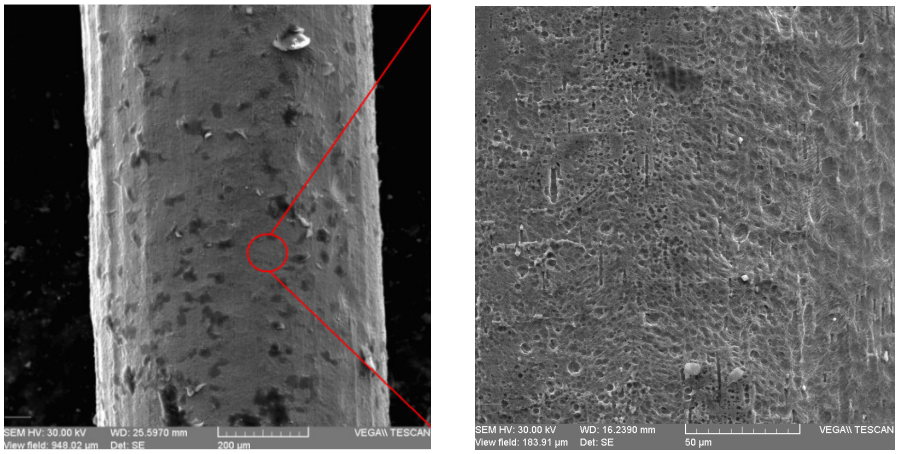

a *b*

Fig. 2 – SEM microscopy of NiTi alloy surface after 34% H_2SO_4+12% HCl solution treated at: 300x (*a*) and 1000x image amplification (*b*).

Tabel 1

Chemical Composition of the NiTi Alloy Surface after the Etching Process with 34% H_2SO_4+12% HCl Solution

Element	AN	series	Net	wt. %	norm. wt.%	norm. %	Error %
Nickel	28	K-series	55590	45.10616	48.47978	35.01133	1.15665
Titanium	22	K-series	84222	39.53445	42.49135	37.61695	1.117648
Oxygen	6	K-series	4771	5.920843	6.36368	22.45776	0.95995
Chloride	11	K-series	803	2.479727	2.665192	4.913955	0.244898
Sum:				93.04119	100	100	

From Fig. 3*b* which is a detail from 3*a* can be observe a degraded surface obtained in this case with loss of material, especially on percentages of titanium based on surface corrosion and especially on appearance of sulfur and chloride chemical elements even in reduce percentages. The formation of TiO layer on the surface is a positive thing at nitinol simple utilization but can became as a negative aspect at the growing of new superficial layers on his surface.

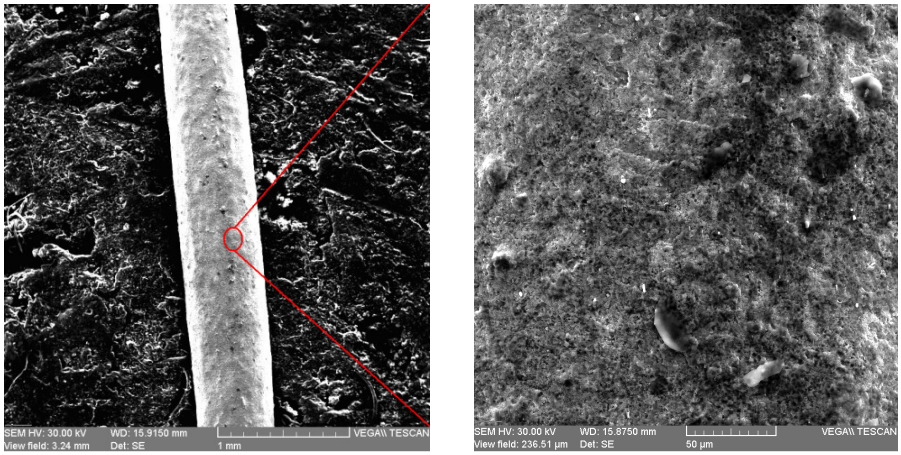

a *b*

Fig. 3 – SEM microscopy of NiTi alloy surface after 48% H_2SO_4+18% HCl solution treated at: 100x (*a*) and 1000x image amplification (*b*).

The area affected, Fig. 3*b*, is homogeneous and fully attacked by chemical solution the sulfur element find on the surface becoming dangerous in any application to obtain thin layers.

Tabel 2

Chemical Composition of the NiTi Alloy Surface After the Etching Process With 48% H_2SO_4+18 % HCl Solution

Element	AN	series	Net	wt. %	norm. wt.%	norm. %	Error %
Nickel	28	K-series	59995	49.25716	48.37716	34.41047	1.259201
Titanium	22	K-series	85391	38.52161	37.8334	32.98836	1.0895
Oxygen	9	K-series	400	11.15141	10.95219	24.06708	3.495825
Sulfur	6	K-series	1939	2.074414	2.037354	7.081523	0.420884
Chloride	11	K-series	276	0.814443	0.799893	1.452569	0.115832
Sum:				101.819	100	100	

Analyzing the surface statement these two attack methods are not considered suitable because of the surface prepared damaged and loss of materials and structural modifications of the surface. Electro-polishing and chemical etchings of Nitinol are known to be efficient for the elimination of defective surface layers and surface oxidizing. Owing to a gain in total energy caused by the differences in the enthalpy of formation of Ti and Ni oxides (Wagman *et al.,* 1982), the preferential oxidation of Ti on Nitinol surface always occurs. As a result, bare Nitinol surfaces are built from Ti oxides with Ni concentrations from 2 to 7 at. %, depending on the electrolytes and regimes employed. Chemical etching and electropolishing of NiTi can be used for surface structuring as well.

Anodizing is an electrolytic passivation process used to increase the thickness of the natural oxide layer on the surface of metal parts. The process is called "anodizing" because the part to be treated forms the anode electrode of an electrical circuit. Anodizing increases corrosion resistance and wears resistance, and provides better adhesion for paint primers and glues than bare metal. Anodic films can also be used for a number of cosmetic effects, either with thick porous coatings that can absorb dyes or with thin transparent coatings that add interference effects to reflected light. Anodizing is also used to prevent galling of threaded components and to make dielectric films for electrolytic capacitors. Anodic films are most commonly applied to protect the alloys although processes also exist for titanium, zinc, magnesium, niobium, and tantalum. This process is not a useful treatment for iron or carbon steel because these metals exfoliate when oxidized; *i.e.*, the iron oxide (also known as rust) forms by pits and flakes, these flakes both fall off as well as trap oxygen-bearing moisture, constantly exposing the underlying metal to corrosion.

Anodization changes the microscopic texture of the surface and changes the crystal structure of the metal near the surface. Thick coatings are normally porous, so a sealing process is often needed to achieve corrosion resistance. The anodization parameters are 55°C solution temperatures, a current of 0.8 mA in a 30 min. period time.

In Fig. 4 SEM microscopies, realized at 1000 and 7500 image amplification times, of Nitinol surface after the first anodizing process are presented as general aspect in Fig. 4*a* and detailed in Fig. 4*b*. As can be see the surface doesn't suffer big modifications comparing with the surface presented in Fig. 1, keeping a nice aspect with small holes on the surface.

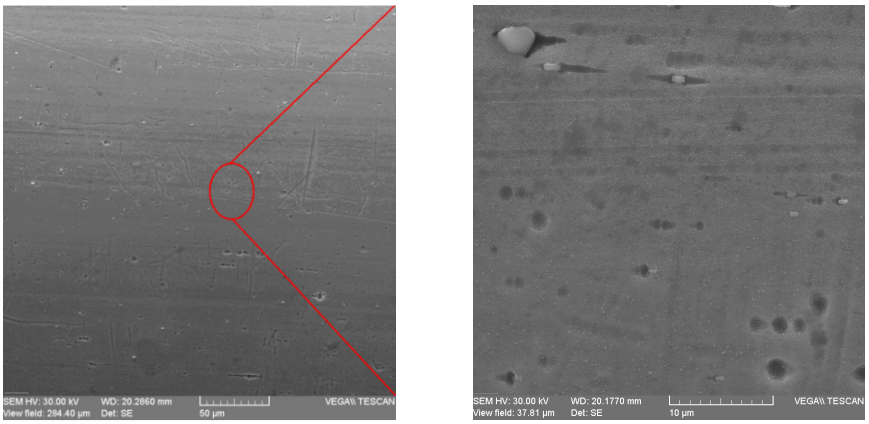

a *b*

Fig. 4 – SEM microscopy of NiTi alloy surface after ANO1 conditions treated at: 1000x (*a*) and 7500x image amplification (*b*).

In Table 3 the EDAX analyze results, like mass or atomic percentages,

are presented having a relatively high Oxygen percentage most based on titanium oxide form on the surface and a reduce carbon percentage. All results were taken from K series with reduce errors in analyze.

Tabel 3

Chemical Composition of the NiTi Alloy Surface After the Etching Process by ANO1 Conditions

Element	AN	series	Net	wt. %	norm. wt.%	norm. %	Error %
Nickel	28	K-series	58599	46.06932	46.12029	32.91557	1.179773
Titanium	22	K-series	88223	40.0286	40.07289	35.05864	1.130774
Oxygen	9	K-series	412	12.55827	12.57217	27.7199	3.891311
Carbon	6	K-series	1211	1.233284	1.234649	4.30589	0.290088
			Sum:	99.88947	100	100	

The experimental results doesn't present an improve of the surface by growing thin films point of view and present bad results for this material after anodizing method, in this experiment conditions, to be used like this without other improvements based on the still reduced percentage of titanium oxide and high percentage of nickel for the alloy surface.

Using second anodizing conditions, 55ºC bath temperature, 0.8 mA activation current and 45 min. period time, the surface is presented through scanning electrons microscopies in Fig. 5 as general view in 5*a* and detail in 5*b*.

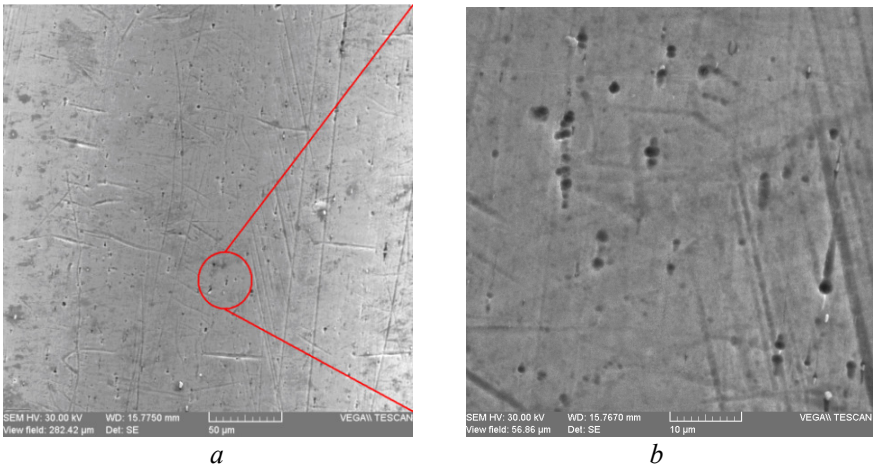

a *b*

Fig. 5 – SEM microscopy of NiTi alloy surface after ANO2 conditions treated at:1000x (*a*) and 7500x image amplification (*b*).

Micro structural results are similar with the previously results with a smooth surface and small holes remarkable only at high magnification images

with dimensions under micron scale.

Chemical results are unsatisfactory as well for the material surface usage in direct contact with the human body (Chuanjun *et al*.). Keeping a high nickel percentage at the surface the material is not improved and the surface is to reduce engraved so applying in this conditions the anodizing is not favorable for the nitinol material.

Tabel 4

Chemical Composition of the NiTi Alloy Surface After the Etching Process by ANO2 Conditions

Element	AN	series	Net	wt. %	norm. wt.%	norm. %	Error %
Nickel	28	K-series	59001	48.56184	51.5174	43.61972	1.242112
Titanium	22	K-series	89438	43.85844	46.52775	48.2921	1.236405
Oxygen	6	K-series	1438	1.842694	1.954844	8.088184	0.403659
			Sum:	94.26297	100	100	

A reduce of the percentage of oxygen, six times smaller than the previous experiment, represent a small percentage of TiO form on the surface layer that is seen by a researcher as a good alternative for thin films deposition (Shabalovskaya *et* al.,). These results are considered very important in chemical improvement of the nitinol surface opening new research opportunities like embedding the TiO thin layer but also to open a path for anodizing process usage in surface preparation.

The research on the surface of nitinol material preparation by chemical methods continued in a further article using other attack solutions also observing the microstructural surface aspect and chemical behavior in the same time with observing the variation of TiO thin layer.

4. Conclusions

Nitinol materials are widely used in the medical field, many applications being in direct contact with the human body. Trying to improve the surface properties of these materials for depositions of superficial thin layers is considered a solution among the increase and evolves of TiO thin layer. Different engraving solution was used, part in this study and other in a further work, to improve the surface of material for adhesion with thin deposited layers the results being based on micrographic analyze (macro and micro areas analyzed) and chemical composition observation at the surface as well. Anodizing methods involving “attack” solutions were analyzed with good results in increasing the TiO superficial layer but with no decrease of nickel percentage at the surface.

REFERENCES

* * * http://www.saesgetters.com/default.aspx?idPage=839

Arndt M., Bruck A., Scully T., Jäger A., Borauel C., *Nickel Ion Release from Orthodontic NiTi Wires Under Simulation of Realistic in-situ Conditions.* J. Mater. Sci., **40**, 3659–3667 (2005).

Bogdanski D., *Untersuchungen zur biocompatibilität and biofunctionalität von implantatmaterialien am beispiel von nickel – titan – formgeda chtnislegierungen.* Dissertation, Ruhr – Universitä Bochum: Germany, 2005.

Chuanjun Huang, Yibin Xie, Limin Zhou, Haitao Huang, *Enhanced Surface Roughness and Corrosion Resistance of NiTi alloy by Anodization in Diluted HF Solution,* Smart Mater. Struct., 18 024003.

Clarke B., Carroll W., Rochev Y., Hynes M., Bradley D., Plumley D., *Influence of Nitinol wire Surface Treatment on Oxide Thickness and Composition and its Subsequent Effect on Corrosion Resistance and Nickel Ion Release.* J. Biomed Mate.r Res., **79A**, 61–70 (2006).

Cui Z., Man H., Yang X., *The Corrosion and Nickel Release Behavior of Laser Surface-Melted Niti Shape Memory Alloys in Hanks Solution.* Surf. Coat .Technol., **192**, 347–353 (2005).

Kobayashi S., Ohgoe Y., Ozeki K., Sato K., Sumiya T., Hirakuri K.., *Diamond-Like Carbon Coatings* on *Orthodontic Archwires*. Diamond Relat. Mater., **14**, 1094–1097 (2005).

Pohl M., Heßing C., Frenzel J., *Electrolytic Processing of NiTi Shape Memory Alloys.* Mater. Sci. Eng., **A378**, 191–199 (2004).

Shabalovskaya S., Anderegg J., Laabs F., Thiel P., Rondelli G., *Surface Conditions of Nitinol Wires, Tubing, and As-Cast Alloys: The Effect of Chemical Etching, Aging in Boiling Water, and Heat Treatment.* J. Biomed. Mater. Res., **65B**, 193–203 (2003).

Shabalovskaya S.A., *Physicochemical and Biological Aspects of Nitinol as a Biomaterial*. Internat. Materials Review, **46**, 1 – 18 (2001).

Shi P., Cheng F., Man H., I*mprovement in Corrosion Resistance of Niti by Anodization in Acetic Acid*. Mater. Lett., **61**, 2385–2388 (2007).

Sui J., Cai W., *Effect of Diamond-Like Carbon (DLC) on the Properties of the NiTi Alloys*. Diamond Relat .Mater., **15**, 1720–1726 (2006).

Wagman D., Evans V., Parker V., Schumm R., Halow I., Bailey S., Churney K., J. Phys. Chem. Ref. Data, Suppl. **2**, 11 (1982).

Wever D., Velderhuizen A., De Vries J., Busscher H., Uges D., Van Horn J., *Electrochemical and Surface Characterization of NiTi Alloy*. Biomaterials **19**, 761–769 (1998).

PROCEDURI EXPERIMENTALE PRIVIND PREGĂTIREA SUPRAFEȚEI METALICE PENTRU PROCESUL DE DEPUNERE DE STRATURI SUBȚIRI (I)

(Rezumat)

Depunerea straturilor subțiri pe substraturi metalice reprezintă o metodă de îmbunătățire a materialelor şi se aplică în mod deosebit celor utilizate în mediul medical în aplicațiile ce necesită contact direct cu corpul uman. Câteva metode chimice de gravare ce include şi anodizarea au fost folosite pentru pregătirea suprafeței unui aliaj cu memoria formei pentru depuneri viitoare de straturi metalice sau nemetalice. Analize chimice, prin spectrometrie de raze X EDAX, şi microstructurale, folosind microscopul cu scanare de electroni SEM, au fost realizate pentru stabilirea câtorva caracteristici de suprafață după ce sau aplicat procesele de modificare a acesteia.

BULETINUL INSTITUTULUI POLITEHNIC DIN IAŞI
Publicat de
Universitatea Tehnică „Gheorghe Asachi” din Iaşi
Tomul LVII (LXI), Fasc. 1, 2011
Secția
ŞTIINȚA ŞI INGINERIA MATERIALELOR

SOME WELDING METALLIC SHEETS METHODS EXPERIMENTAL RESULTS

BY

DRAGOŞ DANĂ, PETRICĂ VIZUREANU*, LUCIAN COSTAN and NICANOR CIMPOEŞU

"Gheorghe Asachi" Technical University of Iaşi,
[1]Faculty of Materials Science and Engineering

Received: February 14, 2011
Accepted for publication: March 28, 2011

Abstract. Welding metallic plate sheets represent an important operation in all machinery manufacturing fields even the materials have different chemical composition, dimensions or properties. Two methods are propose and analyze for welding process based on laser and braze welding. Scanning electrons microscope and EDAX detector were used to characterize the weld line by micro-structural and chemical point of view. Microstructural analysis concentrated on the weld line area present reduces dimensional variation and a modification of the materials surface smoothness. Chemical elements distribution exhibits an increase of carbon percentage on the weld line and a decrease of iron in the same time and area.

Key words: braze welding, laser, scanning electrons microscopy.

1. Introduction

For weight and cost reduction, the technology of tailor welded blanks is a promising technology for automotive, aerospace sectors and vehicle industry.

*Corresponding author; *e-mail*: peviz2002@yahoo.com

In manufacturing of TWBs, a structural part or product is made up by joining several metal sheets of possibly different thicknesses, materials, and surface coatings. The reason is that the joining (welding) is performed prior to forming. The possibility of having different sheets of different thickness, strength, and material properties enable the designer to distribute the material optimally. Optimal distribution of the material, indeed, means lighter structures, higher strengths, and joining before forming results in lower production costs (Gaied *et al*., 2007).

Braze welding is a procedure used to join two pieces of metal being very similar to fusion welding. The filler metal is distributed onto the metal surfaces braze welding usually requires more heat than brazing, by tinning. Braze welding often produces bonds that are comparable to those made by fusion welding without the destruction of the base metal characteristics (Vorob'ev *et al*.) Braze welding result obtain through a SEM analyze is presented in Fig. 1 (www.mtalabs.com).

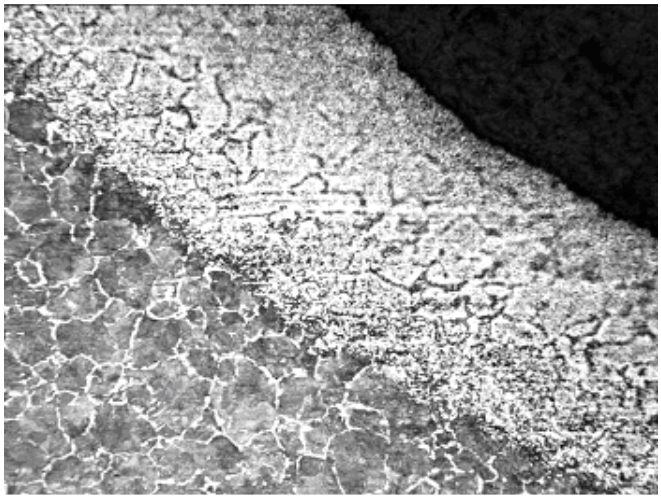

Fig. 1 – SEM image of a braze welded surface (www.mtalabs.com).

Braze welding has many advantages over other welding methods like fusion. It allows you to join dissimilar metals, to minimize heat distortion, and to reduce extensive preheating. Another side effect of braze welding is the elimination of stored-up stresses that are often present in fusion welding. This is extremely important in the repair of large castings.

The edges of the thick parts can be beveled by grinding, machining, or filing. It is not necessary to bevel the thin parts (one-fourth inch or less). The metal must be bright and clean on the underside as well as on the top of

the joint. Cleaning with a file, steel wool, or abrasive paper removes most foreign matter such as oil, greases, and oxides. The use of the proper flux completes the process and permits the tinning to occur (Taban *et al.,* 2010; Pasic *et al.,* 2007). After you prepare the edges, the parts need to be aligned and held in position for braze welding process. This can be done with clamps, tack welds, or a combination of both. The next step is to preheat the assembly to reduce expansion and contraction of the metals during welding. The method you use depends upon the size of the casting or assembly (Uzun *et al.,* 2005).

In this study experimental results of two metallic sheets welding by laser are presented in order to compare the obtained surface with braze welded surface.

2. Experimental Details

The surfaces of the metal must be cleaned for capillary action to take place. When necessary, chemically clean the surface by dipping it in acid. Remove the acid by washing the surface with warm water. For mechanical cleaning, you can use steel wool, a file, or abrasive paper.

One way to follow the influence of the weld line over de forming characteristics is to investigate what is happening in the weld line area from the metallographic and chemical point of view. Energy dispersive X-ray spectroscopy (EDX) is an analytical technique used for the elemental analysis or chemical characterization of a sample having based on the software facilities different analysis modes like Line, Point or Mapping.

3. Experimental Results

The steel sheet named FeP05MB has the thickness of 0.75mm and the other steel sheet named SPE220BH has the thickness of 0.7mm. In Fig. 2 microscopy analyze of the welded area are presented characterizing by micrometer measurements the weld line evolution. From Fig. 2 *a* can be observe different thicknesses between 50 and 500 μm of the cordon and a near modify area exemplify in detail in Fig. 2 *b*.

In Fig. 2 *c* a light intensity distributions on the welded area is presented on a 2.2 mm line passing to weld cordon as well and were can be observe a decrease of intensity similar to a hole fact that represent a surface modification in the welded area as roughness property.

In Fig. 3 a chemical elements distribution is presented on a 1.2 mm line that includes both metallic materials and the welded area. The main

results are given by the iron decrease in the connected area and in the same time the carbon increase.

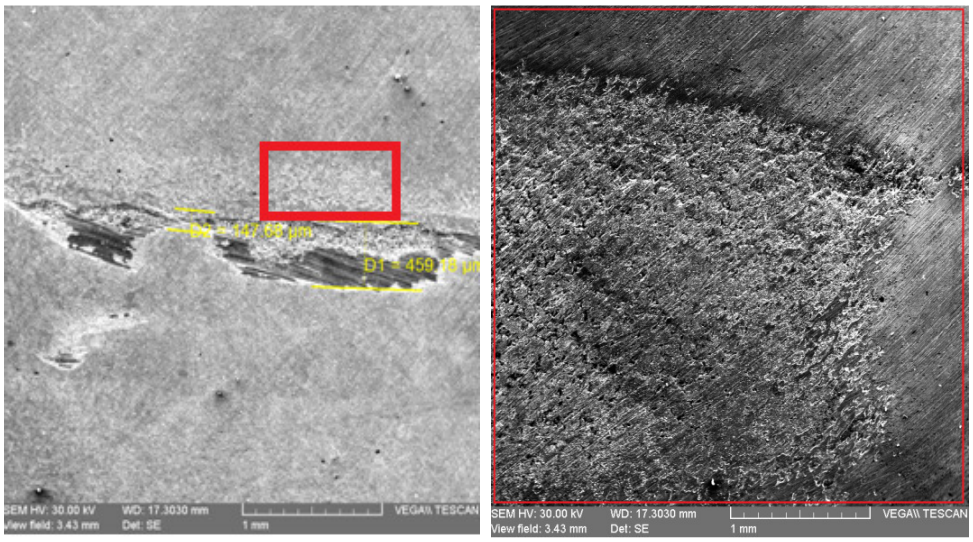

a *b*

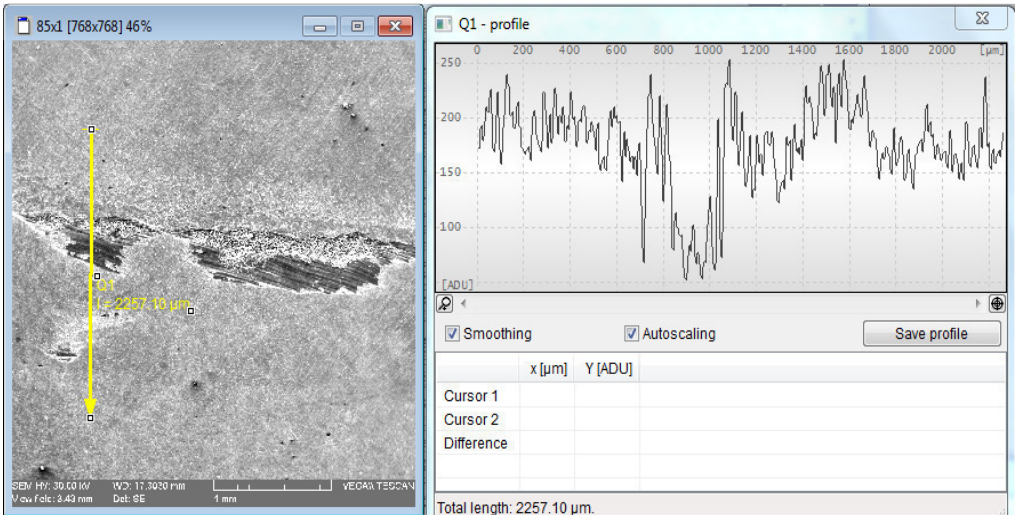

c

Fig. 2 – SEM microscopy of the welded area: *a* – microscopy at 250x with welding cordon and a near area presented in; *b* – and *c* – surface morphology on the welded area.

Fig. 3 – Chemical elements distributions on a 1.2 mm line.

Same chemical elements variation is observe on the mapping mode distribution presented in Fig. 4 were carbon agglomeration on the welded cordon can be seen.

The distribution analyze were made on a 2.56 mm^2 area following the iron, manganese and carbon elements evolution.

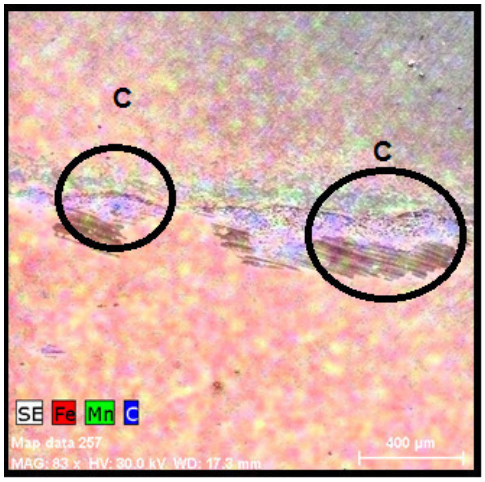

Fig. 4 – Chemical elements distribution on a selected area by mapping of iron (Fe), manganese (Mn) and carbon (C) with selected areas of C agglomeration.

The manganese element is fine distributed in both materials with a higher presence at the upper part of the cordon based on the higher percentage of manganese on the top material.

4. Conclusions

Microstructural characterization of the laser welded area give a dimensional variation of the weld cordon between 50 and 500 μm and evidence a roughness modification in the connection area. Chemical investigations mark a loss of iron percentage on the weld line in the same time with a gain of carbon that seems to agglomerate on the entire welded cordon.

The forming characteristics are significantly reduced in the stretching area of the forming limit diagram, corresponding to axial strain. This means that welded assemblies will extend less before failure when an axial force (along the weld line) is applied.

Acknowledgements. This paper was realised with the support of POSDRU CUANTUMDOC "DOCTORAL STUDIES FOR EUROPEAN PERFORMANCES IN RESEARCH AND INOVATION" ID79407 project funded by the European Social Found and Romanian Government.

REFERENCES

*** http://www.mtalabs.com/Welding_And_Brazing.html

Gaied S., Roelandt J-M., Pinard F., *Numerical and Experimental Investigations in Twbs Formability*, J. of Material Processes and Technology, 908, 1463-1468 (2007).

Pasic O., Hajro I., Hodzic D., *Welding of Dissimilar Metals-Status, Requirements and Trends of Development*. Weld World, **51**, 377–384 (2007).

Taban E., Gould J.E., Lippold J.C., *Dissimilar Friction Welding of 6061-T6 Aluminum and AISI 1018 steel: Properties and Microstructural Characterization.* Mater. and Design. **31**, 2305–2311 (2010).

Uzun H., Donne C.D., Argagnotto A., Ghidini T., Gambaro C., *Friction stir Welding of Dissimilar Al 6013–T4 To X5CrNi18–10 Stainless Steel.* Mater. Des., **26**, 41–46 (2005).

Vorob'ev Yu.S., Chernobryvko M.V., Kolodyazhnyi A.V., Kruszka L., *Analysis of the Process of Explosion Braze-Welding of Heat Exchanger Tube Plates*.

REZULTATELE EXPERIMENTALE ALE UNOR METODE DE LIPIRE A PLĂCILOR METALICE

(Rezumat)

Lipirea plăcilor metalice reprezintă o operație importantă în toate domeniile conexe obținerii de maşini chiar dacă materialul prelucrate prezintă proprietăți chimice şi fizice diferite. Două metode de conectare sunt propuse şi analizate pentru procesul de

lipire pe bază de laser şi de brazare. Microscopul cu scanare de electroni şi detectorul EDAX au fost folosite pentru a caracteriza cordonul de sudură din punct de vedere microstructural şi chimic. Analizele microstructurale bazate pe linia de sudură prezintă variaţii ale cordonului de mici dimensiuni cât şi o modificare a stării suprafeţei în această zonă. Distribuirea elementelor chimice prezintă o creştere a procentului de carbon pe linia de sudură colaborată cu o descreştere a procentului de fier.

BULETINUL INSTITUTULUI POLITEHNIC DIN IAŞI
Publicat de
Universitatea Tehnică „Gheorghe Asachi" din Iaşi
Tomul LVII (LXI), Fasc. 1, 2011
Secția
ŞTIINȚA ŞI INGINERIA MATERIALELOR

INTERFACE ANALYZE OF A COMPOSITE MATERIAL WITH SHAPE MEMORY ALLOY MATRIX

BY

ALEXANDRU ENACHE, IULIAN CIMPOESU, SERGIU STANCIU, ION HOPULELE, MIHAI AXINTE and NICANOR CIMPOESU*

"Gheorghe Asachi" Technical University of Iaşi,
Faculty of Materials Science and Engineering

Received: February 14, 2011
Accepted for publication: March 28, 2011

Abstract. A new composite material made by a copper based shape memory alloy as a matrix and an arch steel material as a reinforcement element was analyzed. Using classical melting methods a composite material was obtained and analyzed concerning the interface between those two involve alloys (memory material CuZnAl and arch steel). Chemical and micro-structural considerations were performed to establish the composite behavior at the interface especially based on homogenization period time modification (between 10 and 360 minutes).

Key words: shape memory alloy matrix, diffusion, metallic interface.

1. Introduction

Since the shape memory alloys first investigations tremendous effort has been infused to the utilization and study of this smart material. Shape memory alloy (SMA) exhibits two related phenomena, shape memory effect (SME) and superelasticity (SE) (Greiner *et al.,* 2005*;* Kato *et al.,* 1994*;* Liu *et al.,* 2007).

*Corresponding author; *e-mail*: nicanornick@yahoo.com

Both are due to reversible phase transformations between two crystal structures, austenite and martensite. Composite structures have been around for many decades, but they are just beginning to see increased use in common structures today. As such there has been increasing interest in producing better, more functional composites and of particular interest are adaptive composites. Adaptive composites are those which have incorporated within their structure some form of "smart" material which can be used to sense the environment surrounding it and to then actuate or control the structure (Krstulovic-Opara *et al.,* 2003).

One type of adaptive composite which is currently under investigation are shape memory alloy composites (SMA-composites), in which SMA elements are usually incorporated into fibers reinforced epoxy composites but similar can be used (the shape memory alloy) as matrix material as well with arch steel reinforcement elements (Tsoi *et al*., 2003).

Accepting the shape memory matrix properties and the mechanical characteristics of the arch wire in this paper is analyzing the metal-metal interface created between the copper and iron based materials of the composite especially after different homogenization time periods.

2. Experimental Details

To obtain the alloy was used a laboratory furnace with a graphite crucible using copper, zinc and aluminum high purity materials with reduce the percentage of iron (Mares *et al*., 1997). The heat treatments were realized on a laboratory Vulcan furnace with good temperature variation control (Cimpoeşu *et al*., 2008).

Chemical composition was determined through sparking spectrometry analysis using Foundry Master equipment (for matrix and reinforcement elements chemical analysis) and EDAX analysis as well for interface study. In this study EDAX software applications were used to determine the chemical variation of the elements on Line, Mapping or Point mode with automatic or element list considerations. Microstructures of the composite in different heat treated states of material were obtained with a scanning electron microscope (SEM) LMH II by Vega Tescan brand using a secondary electrons (SE) detector.

3. Experimental Results

A composite material who used a shape memory alloy ($Cu_{75}Zn_{20}Al_5$) as a matrix and an Rp5 steel material as reinforcement fiber.

Shape memory composite material general view is presented in Fig. 1 with oxidation amounts, especially on the steel fiber and expressing a nice continuous interface between those two metallic materials involve in a

compound. Image was taking with a 250x power amplification obtaining a 200μm scale.

After the pouring of the matrix the composite material necessity is a homogeneity heat treatment that concern heating the material to 750°C, a maintaining period (10, 60 and 360 min.) followed by a cooling to room temperature with the furnace. In Fig. 2 are presented the composite material detail of them interfaces for material maintained 10 min. in *a*, maintained 60 minutes in *b* and 360 min. in *c*.

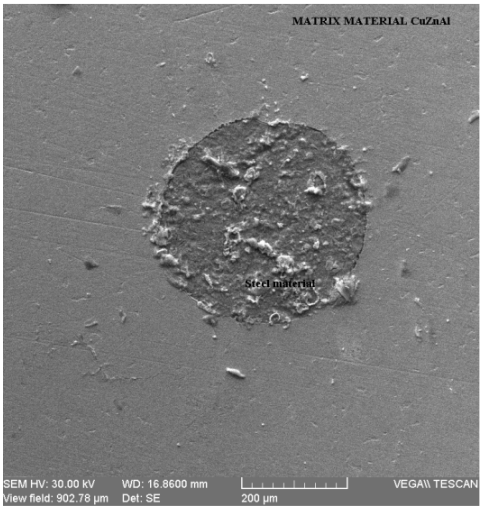

Fig. 1 – General view of a composite material with shape memory matrix and steel reinforcement fiber.

It can be observing the interface modification with increasing of maintaining period and appearing (forming) a different structural or chemical layer between the matrix and the fiber, especially in the last treatment case.

Dimensional measurements done on the interface results in these three cases shows some formation centers of a new layer on the border between materials in the first case that are small and rare and, which grow with the maintaining time, Fig. 2 *b* at 2-3 μm to 8-10 μm in the last case.

One of the chemical elements affected by the heat treatment maintaining period is aluminum which distribution exemplifies in Fig. 2 *d*, *e* and *f* can be observing the interface layer formation for different maintaining periods at the beginning just with some reduce and uniform presence in the matrix, Fig. 2 *d* few agglomerations of aluminum in Fig. 2 *e* for sixty minutes maintaining time and perfect contoured and formed layer at the interface in 2 *f* (formation of a bigger dimensional interface based on chemical reactions or diffusion).

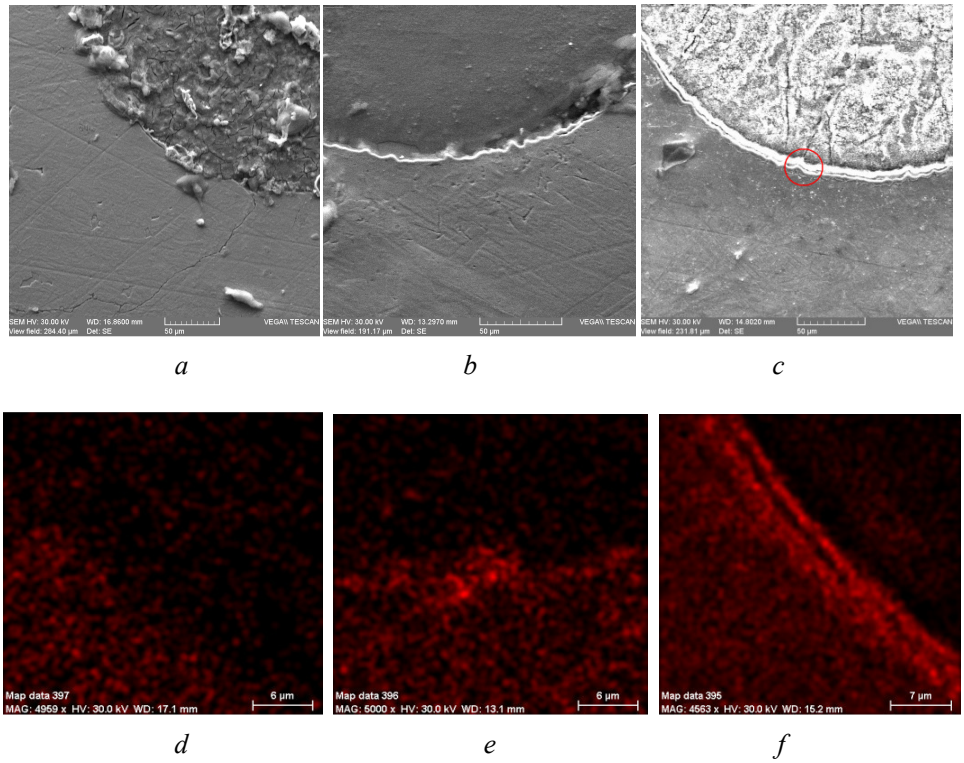

a *b* *c*

d *e* *f*

Fig. 2 – A composite materials with shape memory alloy matrix microstructures: *a*) after 10, *b*) 60 and *c*) 360 minutes heat treatment homogenous time and the aluminum element distribution in similar cases for *d*), *e*) and *f*).

In Fig. 3 two types of an interface that can be created can be observed and analyze, in the left the reactive interface type which occurs in the second part of the creating border process exemplifies by a mapping aluminum element diagram and also a line distribution on a selected area and the diffusion type presented in the right part of the image 3 and exemplify by a Line distribution of elements in the right down part of the figure.

These two processes occurred simultaneous and form the interface between matrix a shape memory alloy and the reinforcement fiber a steel material.

In Fig. 4, a detail of Fig. 2 *c* marked with a red color circle, is presented at a 5000-time amplification power the microstructure of the composite interface of a sample heat treated for homogeneity time of 360 min. Is observing a separation of the interface based on diffusion and chemical reactions that occur based on a thermal contribution of the heat treatment.

In Fig. 2 are selected two points on interface, one on the reinforcement part (one) and second on the matrix part (two) and the chemical analysis do in

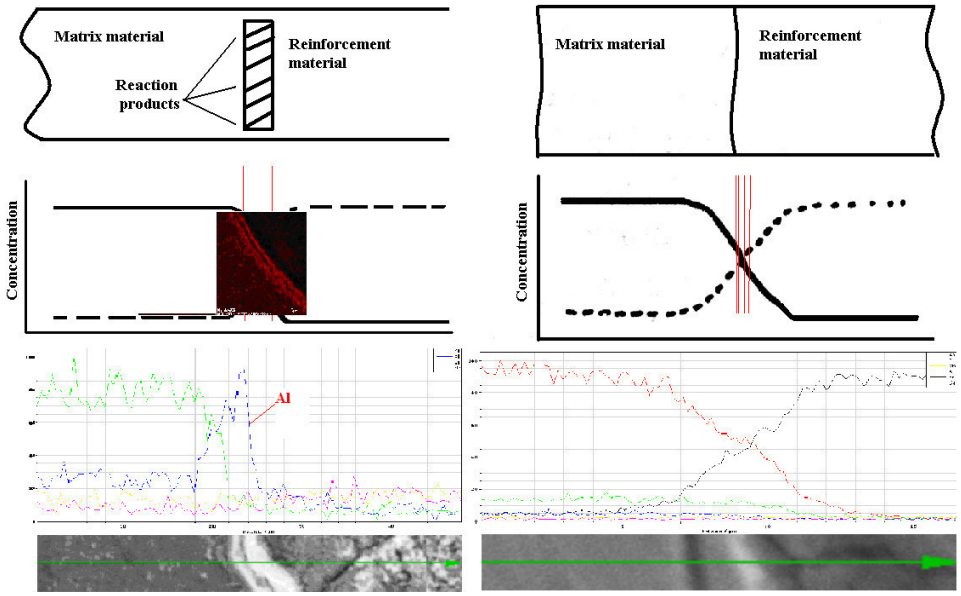

Fig. 3 – Interface behaviors on a metallic composite case with shape memory alloy matrix.

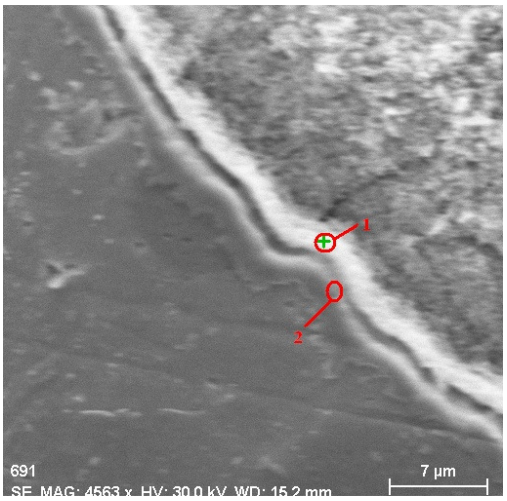

Fig. 4 – Detail of interface in the 360 minutes heat treated sample - red selected area from Fig. 2*c*.

these points has the results in Table 1 and 2. In these two points is following the evolution of most important elements that are based both alloys that form the composite material like a matrix made by copper, zinc and aluminum and the arch steel wire made of iron, manganese, silicon and non metallic carbon.

Table 1
Chemical Composition of the Interface Layer in Point One Selected in Fig. 4

Element	Net	wt. %	norm. wt. %	norm. at. %	Error in %
Iron	99591	65.99347	69.45526	56.30172	1.704284
Aluminum	18314	19.60635	20.63483	34.62187	1.031794
Copper	4568	5.076885	5.343201	3.806533	0.173997
Silicon	2183	2.07882	2.187868	3.526593	0.13665
Zinc	1294	1.565026	1.647122	1.140331	0.085399
Manganese	1278	0.695245	0.731715	0.602956	0.087863
Sum:			95.0158	100	100

Table 2
Chemical Composition of the Interface Layer in Point Two Selected in Fig. 4

Element	Net	wt. %	norm. wt. %	norm. at. %	Error in %
Iron	117534	70.82367	73.16777	65.16941	1.82436
Aluminum	10575	12.32013	12.72789	23.46462	0.668946
Copper	9165	10.36535	10.70842	8.382258	0.30521
Zinc	2022	2.426492	2.506804	1.906921	0.108126
Manganese	1123	0.556745	0.575172	0.520773	0.082693
Silicon	328	0.303881	0.313939	0.556015	0.050266
Sum:		96.79627	100	100	

We observe some differences in chemical composition results, even the both points are on interface and relatively close one to the other, manifest by a bigger percentage (mass and atomic) of iron in point two and aluminum in point one that are contrary to the position near the closest material like brass and steel. We are observing a different percentage of aluminum in the interface (only 5% in a matrix and more than 10 or even 20 in the interface), a smaller percentage of zinc compared with the matrix in point one and two.

4. Conclusions

A metallic composite based on a SMA matrix was obtained and analyze by interface modification with homogeneity heat treatment maintaining period. An interface based on iron, aluminum, and copper and zinc compounds is forming with increasing of the maintaining period of homogeneity treatment with sizes of 8-10 μm that improve the bond between matrix and the reinforcement elements. Diffusion and reactive interface growth processes were observed to contribute to a final obtained border exemplify by element distribution mapping and evolution.

Acknowledgements. This paper was realised with the support of POSDRU CUANTUMDOC "DOCTORAL STUDIES FOR EUROPEAN PERFORMANCES IN RESEARCH AND INOVATION" ID79407 project funded by the European Social Found and Romanian Government.

REFERENCES

Cimpoeşu N., Enache A., Stanciu S., Nejneru C., Achiţei D., Hopulele I., *Composite Shape Memory Materials Obtaining Methods.* Simpozionul International ARTCAST 2008, Galaţi, 293-296 (2008).

Greiner Christian, Oppenheimer Scott M., Dunand David C., *High Strength, Low Stiffness, Porous NiTi with Superelastic Properties*. Acta Biomaterialia **1**, 705–716 (2005).

Kato H., Dutkiewicz J., Miura, S., *Superelasticity and Shape Memory Effect in Cu-23at.AI-7at%Mn Alloy Single Crystals*. Acta Metall. Mater., 42, 1994, 1359-1365.

Krstulovic-Opara N., Nau J., Wriggers P., Krstulovic-Opara L., *Self-Actuating SMAHPFRC Fuses for Auto-Adaptive Composite Structures*. Comput. Aided Civil Infrastructure Eng., **18**, 78–94 (2003).

Liu J., Li J.G., *Microstructure, Superelasticity and Fracture Behavior in Magnetic Shape Memory Co–Ni–Ga–Fe Alloys with Two-Phase Structures*. Scripta Materialia **56**, 109–112 (2007).

Mares M.A., Carcea I., Chelariu R., Roman C., *Mechanical and Tribological Properties of Aluminium Matrix Composites After Ageing Treatments*. Euromat 97 - Proceedings of the 5th European Conference on Advanced Materials and Processes and Applications: Materials, Functionality & Design.- Metals and Composites, **1**, 423-426 (1997).

Tsoi K. *et al*., *Impact Damage Behavior of Shape Memory Alloy Composites*. Mater. Sci. Enf., **342**, *1-2*, 207-215 (2003).

ANALIZA INTERFEŢEI UNUI MATERIAL COMPOZIT CU MATRICE DIN ALIAJ CU MEMORIA FORMEI

(Rezumat)

Un material compozit nou cu matrice din aliaj cu memoria formei pe bază de cupru şi element de ranforsare un oţel de arc a fost analizat. Utilizând metode clasice de topire şi turnare un material compozit a fost obţinut şi analizat din punctual de vedere al interfeţei dintre cele două aliaje implicate în compozit (un aliaj cu memoria formei CuZnAl şi un oţel de arc). Consideraţii chimice şi microstructurale au fost realizate pentru stabilirea comportamentului materialului compozit la interfaţă în funcţie de timpul de tratament de omogenizare (între 10 şi 360 de minute).

BULETINUL INSTITUTULUI POLITEHNIC DIN IAŞI
Publicat de
Universitatea Tehnică „Gheorghe Asachi” din Iaşi
Tomul LVII (LXI), Fasc. 1, 2011
Secția
ŞTIINȚA ŞI INGINERIA MATERIALELOR

COMPOSITE MATERIALS – A REVIEW

BY

RALUCA MARIA FLOREA* and IOAN CARCEA

"Gheorghe Asachi" Technical University of Iaşi,
Faculty of Materials Science and Engineering

Received: March 24, 2011
Accepted for publication: March 28, 2011

Abstract: This paper presents an overview of composite materials. The main aim was to evaluate both the development and the requirement of those materials. The subject is treated during four chapters. In the first chapter is given an itinerary of composite materials from the time of ancient Egypt until today. In the second chapter are specified areas of applications with a sampling of dental adhesive composites. Chapter three is reserved for processing techniques of materials whit polymer, ceramic, carbon and metal matrix composites. This summary concludes with overall conclusions and a perspective view of composite materials.

Key words: cast, composite, matrix.

1. Introduction

Between the constituents of the universe, solar system, the land and any amount material are interactions that alter the characteristics of the whole system so it can be said that we live in a world of composite materials (Carcea, 2008). As a composite material is considered any material composed of two or more constituent interacting with each other to give

*Corresponding author; *e-mail*: raluca.m_florea@yahoo.com

birth to a completely new material with different properties and, in general, superior to any of them (Carcea, 2008; Banu *et al*., 2001).

Based on the patterns of nature: plants are reinforced with cellulose fibers, animal tissues are reinforced with fibers of collagen, elastin or keratin etc we can find examples of composite materials produced by people since ancient times: cellulose fiber reinforced with clay in ancient Egypt, counseling sand with chalk and volcanic tuff in Roman Empire, construction reinforcement with iron rods etc. Vessel at the museum in London, made in Scotland in the year 900 with glass fiber reinforced resin, foreshadows the current state of reinforced organic fiber composites. After the 1942 composite resin - glass fiber was used to conduct the first boat, followed by the aircraft and then was used for electrical components. The first boron and carbon fibers, with high tensile strength, occurred at the end of 1960, and composites made with these materials were considered advanced materials and from 1968 is used to manufacture many aircraft components. Ceramic matrix composite materials were introduced in 1970. Kevlar fibers were made by Dupont in 1973. Since the end of 1970s the need of composite materials and in particular the fiber-reinforced expanded into areas: aviation, automobiles, boats, sports, medicine etc. Benefits for these materials conquer product market are: low weight compared to conventional materials, high wear resistance, corrosion, mechanical properties in accordance with the operational demands of the product (Banu *et al*., 2001).

Since processing of composite materials is difficult and complex operating conditions are rigorous, and mechanical properties, physical, chemical, electrical, magnetic, etc. are dependent on the arrangement and compatibility of components, it is necessary to develop multidisciplinary research programs.

2. Fields of Use

The use of composite materials has a crucial role in increasing their specific properties and these properties which can be adapted to operating conditions. Because they have very wide applicability the following table aims to provide an insight into the way how are these used.

From this point of view an interesting example to note, is the use of composites materials in dentistry. If the first resins composite (*e.g.* methacrylate) were used after 1930, with auto curing resin dental fillings were used in the next decade.

According to the statements of Rafael L. Bowen (Gregory *et al.,* 1992) from 1962, resin composites reinforced with inorganic particles treated with silane gives good adhesion to the wall of the tooth, minimum polymerization shrinkage, increased hardness and mechanical load borne. A real breakthrough occurred in 1970 when were introduced the dental composites

Table 1
Applications of Composite Materials

Composite Materials – Fields of Use	
Mechanical engineering	- agricultural machinery; hoists; vehicles; rolling stock; - aircraft (glider, helicopter, aircraft, spacecraft): empennage; wings; propeller; hull; deflector; jet propulsion; black boxes; heat shield; - shipbuilding: boats; yachts; submarines; minesweeper.
Construction	- tanks, roofing, carpentry, cooling towers, pipes, tubes, profiles, patterns, framings, facade panels, movable bridges.
Medicine	-cardiac implants; orthopedics: prostheses; dentistry: implants.
Optical	- telescope; binoculars; microscopes; glasses frames.
Energy	- wind generator; turbine blades; heat and radiation shields.
Electronic	-computers; printers; televisions; radio; robots .
Sport	- bob; ski; bowling lanes; swimming pools; tennis racquets; pole vault.
Chemistry	- chemical equipment; pressure vessels; catalysts.

which polymerize under the action of light. Posterior dental treatments with modern hybrid composites are currently recognized by the German Association for Dental, Oral and Maxilla-facial and German Dental Association that continuous treatment (Willems *et al.,* 1993).

a *b*

Fig. 1 – Composites used in dentistry (Gregory *et al.,* 1992): *a* – dental composites reinforcing macro-particles can degrade easily and are more difficult to polishing; *b* – dental composite reinforced with micro-particles in excess are viscous and difficult to model.

3. Composite Materials Processing Techniques

Depending on the nature of matrix composite materials are classified as: polymeric, ceramic, carbon and metal. On this classification is based the following brief overview of methods and manufacturing.

3.1. Processing Techniques of Polymer Matrix Composites

The most important methods of manufacturing polymer-based composites are described below (Mareş, 2002; Asthana *et al.,* 2006; Nedelcu *et al.,* 2009).

- *gravity casting*: free fall casting of resins-particles (short fibers) to obtain large parts of thermosetting composites;

- *under pressure casting*: consists in injecting liquid matrix of fiber or particles in a premould placed in a metal mold;

- *forming by contact*: consist in use of open lasts on which are enforcing successive layers of polymeric material and reinforcing elements;

- *forming by simultaneous spray*: for this process is uses a device like a spray gun, wherein the matrix material is mixed with particles or chopped fibers to the desired length;

- *forming in sack*: consist on placing above the model of fibers and resins successive layers where is fixed an elastic and durable film (bag) tightly around the edges, through a pressure box or a metal frame, and after application of pressure, namely depression, is heated to polymerize;

-*forming by vacuum injection*: for process are used two metal moulds perfectly calibrated, between this mould is placed the reinforcing material, interior space is then evacuated, that so the resin (matrix) is brought forcibly to fill the intervals between the reinforcing elements;

- *cold pressing*: for this process are used two metal moulds in which in which the mixture of constituent is maintained under pressure until strengthen its complete;

- *hot pressing*: the materials are reticulated at warm in closed moulds, and the final thickness of the work piece is adjusted by the number of layers of introduced impregnated fabrics, after heat treatment the material is left to cool in the mold under pressure;

- *formation by continuous stratification*: it is used a furnace in which the matrix is reticulated and the material is specialized and it is cut at the wanted sizes;

- *formation of honeycomb core panels*: panels consisting of several layers joined together and secured in the form of honeycomb, process involves two steps: placing components cut to desired size and thermal formation of the panel itself, on a hot press platens at 170 ÷ 190°C and pressures of 2÷4 Mpa.

3.2. Processing Techniques of Ceramic Matrix Composites

The main technological methods of production ceramic composite are (Mareş, 2002; Asthana *et al.,* 2006; Russo, 2006; Leon-Patiño *et al.,* 2005):

- mixing, casting and sintering of components;

- infiltration of a matrix material slips into a preformed with reinforcing elements;

- producing a ceramic paste, which includes reinforced elements, then apply under pressure casting method;

- deposition of vaporized ceramic matrix into a reinforced elements premould.

Currently is using dispersed reinforcing elements like monocrystalline filaments (*e.g.* SiC) or like particles (most common are those of TiN or graphite).

3.3. Processing Techniques of Carbonic Matrix Composites

This type of composite has both matrix and reinforcing elements consisting of varieties of carbon and exceptional properties in terms of resistance to shock and abrasive wear.

The main method of producing carbon composites consist of successive impregnation of carbon fiber with precursor materials (synthetic resins, tar, asphalt, etc.). After compaction, the fiber packages are subject to thermal treatment and to hardening and solidification of the matrix (Carcea, 2008; Mareş, 2002):

- carbonization involves preheating the compacted mixture at 700 ÷ 900°C in an inert atmosphere, with the removal of hydrogen and volatile substances, plus a final heating at approx. 1500°C;

- graphitization includes the same preliminary stages but the final heat of the compacted material is at 2800 ÷ 3000°C.

During these stages is produced matrix material part vaporization and at the surface pores appear. To obtain a more compact material, porosity is filled by a new impregnation material precursor, and then repeats the carbonization and graphitization steps.

3.4. Processing Techniques of Metal Matrix Composites

Depending on the state of matrix incorporating reinforcing elements, processes for obtaining these composites can be divided into (Carcea, 2008; Asthana *et al.,* 2006; Zgură *et al.,* 2000; Nedelcu *et al.,* 2009): processing technology of composites from liquid or semisolid matrix, derived from the processes of casting alloys; production and processing technologies in solid matrix, derived from powder metallurgy; spray deposition technologies.

a) *Technologies Derived from Casting Processes*

Technologies derived from casting processes have emerged as the most cost-effective methods of implementing many variations and can replace

conventional products with similar products molded of composites materials with high performance. These technologies are classified in:

- *under gravity casting (gravity casting)* (Nedelcu *et al*., 2009): consists in pouring the matrix-reinforcement element mixture made by intense mechanical agitation - Vortex method – in the crucible melting facility;

- *centrifugal casting*: centrifuged the alloy-reinforcing suspension throughout the casting and solidification of the mixture;

- *campocasting*: is based on grains finishing process at the semi-solidified alloy casting, when appear the phenomenon called "dendrites remelting" (Ienciu *et al*., 1985);

- *infiltration casting*: is based on the introduction of the liquid alloy in the gaps of the reinforcing elements premould and it can happen in four technological options (Mareş, 2002; Asthana *et al.,* 2006; Leon-Patiño *et al.,* 2005; Zgură *et al.,* 2000): by capillarity; by pressurized injecting of liquid matrix; by vacuum form; by forced immersion of fibers in molten metal;

- *squeeze casting* (Carcea, 2008): casting of alloy-reinforcing suspension in metal molds and application of high pressure (approx. 2000 daN/ cm^2) during solidification;

- *casting in space*: consist in melting and solidification in space of special composite materials, obtained previously in normal.

b) *Production and Processing Technologies in Solid Matrix*

a) Manufacture of metal composite materials derived from powder metallurgy technologies

These technologies allow the production of finished parts as close, with different concentrations and combinations of components, including reactive coupling components (*e.g.* Ti/SiC_p (Caron *et al.,* 1990)) and mechanical properties superior to those obtained by casting technologies (Asthana *et al.,* 2006; Russo *et al.,* 2006; Barekar *et al.,* 2009; Ralph *et al.,* 1997).

The disadvantage is that the process is slow, expensive and requires additional safeguards (e.g. powders of Mg and Al are flammable) (Ibrahim *et al.,* 1991; Srivatsan *et al.,* 1991; Gupta *et al.,* 1993).

b) Methods based on solid state diffusion components

Consist in making a contact between areas of two distinct materials at high temperature by applying a mechanical pressure. These two conditions favor the diffusion between those two materials. Pressure can be lowered, in which case the process must be conducted in a vacuum or controlled atmosphere or high in cases where intentional deformation of the composite is desired (Mareş, 2002; Asthana, *et al.,* 2006; Russo, 2006). These methods are generally applicable to produce composites consisting of layers with reinforcing elements in fiber form.

c) *Spray Deposition Technology*

Spray deposition process can be considered an intermediate technology between the processes of casting and powder metallurgy based on because combines the mixing operations between the matrix of fine liquid particles form and complementary material with solidification and consolidation processes (Caron *et al.,* 1990; Ralph *et al.,* 1997).

Spray deposition or thermal spray process is applied in two variants:

a) *inert gas spray deposition*: this method, known as the Osprey process (Caron *et al.,* 1990; Ralph *et al.,* 1997); Ibrahim *et al.,* 1991) consists in the decay of liquid matrix in very fine drops under the action of an inert gas (usually argon) and in the injection of additional material (reinforcement material) particles, in a common field;

b) *plasma jet deposition*: is based on melting and disintegration of the alloy matrix in very fine droplets form in a plasma jet created by heating an inert gas in an electric arc to high temperatures ($\geq$ 10000 K). The arc is established between the anode represented by matrices and a water-cooled copper cathode (Zgură *et al.,* 2000).

4. Conclusions and Perspectives

It can be said that composite materials opened the possibility of a new rival philosophies in the design of materials, because these materials allow the achieving of an ideal composition at desired material, simultaneously with the final design of optimal structure in an interactive process.

Polymer matrix composites are manufactured using very different methods, which allow the designer of the material to choose that option which is closely at the global properties of the final product specific application requirements.

In the case of ceramic composites, additional materials are often in the form of short or long fibers. Now are used ceramics with reinforcing elements dispersed like particle or crystal filaments.

For carbon matrix materials, more often, reinforcing elements have long fibers form. If the fibers are unidirectional it is obtained the higher tensile strength. If the fibers are arranged in two directions, the material his behavior is close to the isotropy. Materials in which fibers are arranged in three directions are nearly isotropic and have high resistance to crack propagation.

Compared to the polymeric, ceramic or the carbonic matrix metal matrix has some advantages related to: ductility and superior mechanical properties, resistance to certain solvents attack, a wider range of service temperatures, better electrical and thermal conductivity, greater resistance to ignition, dimensional stability, good capacity for processing, low porosity etc.

In future we would like that with a specific design of products and technologies to obtain the isotropic and anisotropic properties of the amount and spatial arrangement to have the highest reliability and performance of technical and economic efficiency. It is also considering contributing to environmental sustainability through research on resource conservation and pollution prevention.

Acknowledgements. This paper was realised with the support of POSDRU CUANTUMDOC "DOCTORAL STUDIES FOR EUROPEAN PERFORMANCES IN RESEARCH AND INOVATION" ID79407 project funded by the European Social Found and Romanian Government.

REFERENCES

Asthana R., Kumar A., Dahotre N.B., *Material Processing and Manufacturing Science*. Academic Press, 2006.

Banu M., Naidim O., Tăbăcaru V., *Materiale neconvenționale.* Edit. Fundației Dunărea de Jos, Galați, **I**, 2001.

Barekar N., Tzamtzis S., Dhindaw B.K, Patel J., Hari Babu N., Fan Z., *Processing of Aluminum-Graphite Particulate Metal Matrix Composites by Advanced Shear Technology*. J. of Materials Engineering and Performance. **18**, 1230-1240 (2009).

Carcea I., *Materilale compozite – fenomene la interfață*. Ed. Politehnium. Iaşi, 2008.

Caron S., Masounave J., *A Literature Review on Fabrication Techniques of Particulate Reinforced Metal Composites*. Fabrication of Particulated Reinforced Metal Composites, Montreal, Canada, 83-88 (1990).

Gregory W.A, Berry S., Duke E., Dennison J.B., *Physical Properties and Repair Bond Strength of Direct and Indirect Composite Resins.* **68**, *3*, 406-411 (1992).

Gupta M., Mohamed F., Lavernia E., Srivatsan T.S., *Microstructural Evolution and Mechanical Properties of SiC/Al_2O_3 Particulate-Reinforced Spray Deposition Metal Matrix Composites*. J. of Material Science. **28**, 2245-2259 (1993)

Ibrahim I.A., Lavernia E.J., Mohamed F.A., *Particulate Reinforced Metal Matrix Composites.* A review. Materials Science Engineering, **24**, 1137-1156 (1991).

Ienciu M., Moldovan P., Panait N., Buzatu M., *Elaborarea şi turnarea aliajelor neferoase special*. Ed. Didactică şi pedagogic, Bucureşti, 1985.

Leon-Patiño C.A., Drew R.A.L., *Role of Metal Interlayers in the Infiltration of Metal–Ceramic Composites*. Solid State and Materials Science, **9**, 211–218 (2005).

Mareş M., *Materiale composite*. Edit. Univ. Tehn. "Gh. Asachi", Iaşi, 2002.

Nedelcu D., Carcea I., Neagu G., Zăgan R., Tăbăcaru L., Predescu C., *Tehnologii de obținere a materialelor compozite*. Edit. Politehnium, Iaşi, 2009.

Ralph B., Yuen H.C., Lee W.B., *The Processing of Metal Matrix Composites – an Overview*. J. of Materials Processing Technology, **63**, 339-353 (1997).

Russo M., *Ceramic and Metal Matrix Composites: Routes and Properties*. J. of Mater. Processing Technology, **175**, 364–375 (2006).

Srivatsan T.S., Ibrahim I.A., Mohamed F.A., Lavernia E.J., *Processing Techniques for Particulate-Reinforced Metal Matrix Composites*. Mater. Sci. Engng., **26**, 5965-5978 (1991).

Willems G., Lambrechts P., Braem M., Vanherle G., *Composite Resins in the 21st Century*. Ed. Quintessence Int, **24**, 641-658 (1993).

Zgură Gh., Severin I., Tonoiu I., *Materiale compozite cu matrice metalică*. Ed. Acad. Române, Bucureşti, 2000.

MATERIALE COMPOZITE−SINTEZĂ

(Rezumat)

Lucrarea prezintă o vedere de ansamblu asupra materialelor compozite şi işi propune ca obiectiv principal să evalueze atât dezvoltarea cât şi necesitatea acestor materiale.

Subiectul este tratat pe parcursul a patru capitole. În capitolul întâi este prezentat un itinerariu al materialelor compozite din vremea Egiptului Antic până în zilele noastre. În cel de-al doilea capitol sunt specificate domeniile de aplicații cu o exemplificare asupra compozitelor adezive dentare. Capitolul trei este rezervat tehnicilor de procesare a materialelor compozite cu matrice polimerică, ceramică, carbonică şi metalică.

Această sinteză se încheie cu concluziile generale şi cu o vedere de perspectivă asupra materialelor compozite.

BULETINUL INSTITUTULUI POLITEHNIC DIN IAŞI
Publicat de
Universitatea Tehnică „Gheorghe Asachi” din Iaşi
Tomul LVII (LXI), Fasc. 1, 2011
Secția
ŞTIINȚA ŞI INGINERIA MATERIALELOR

THE RATE OF DRAWING INFLUENCE DURING THE TUBES PROCESSING WITHOUT INSIDE GUARD IN ULTRASOUND FIELD

BY

BOGDAN-LUCIAN GAVRILĂ*, MIHAI SUSAN, ELENA CHIRILĂ, DRAGOŞ-CRISTIAN ACHIȚEI and BOGDAN COJOCARIU

"Gheorghe Asachi" Technical University of Iaşi,
Faculty of Materials Science and Engineering

Received: February 25, 2011
Accepted for publication: March 28, 2011

Abstract: The paper gives information about the rate of drawing, (v_{tr}), influence during the tubes processing without inside guard in ultrasound field / UVD system, when the die is placed in the antinodes of the waves oscillation and it is activated along the drawing direction. This the case of the tubes made of metallic materials which are strong hardened by cold plastic deformation.

Key words: tube, ultrasounds, oscillator system, rate of drawing, ultrasounds surface effect.

1. Introduction

The paper analysis the rate of drawing, (v_{tr}), influence to the force of the tubes processing without inside guard, "ultrasonic vibration drawing" / UVD system; the tubes made of metallic materials which are strong hardened

*Corresponding author; *e-mail*: bgdnlcn@yahoo.com

by cold plastic deformation. The object of the paper is to characterize, from the technological point of view, the new process in the tubes manufacturing, by drawing without inside guard in UVD system, when the die is placed in the antinodes of the waves oscillation and it is activated along the drawing direction, considering the rate of drawing, (v_{tr}), as the analyzed parameter. When the die is placed in the antinodes of the waves oscillation and it is activated along the drawing direction, the plastic deformation process generates "the ultrasound surface effect" or "the reduction of the metal – tool contact friction effect" based on the Severdenko's model, (Severdenko, *et al.,* 1990; Susan, 2008).

Severdenko and Miskevici have shown that, due to the composition of the two rate vectors, ($\vec{v}_v$ and $\vec{v}_a$), the resultant vector of the relative rate will change the direction of P point motion, (placed at the metal – tool contact surface), in this way: during $T/2+2t_1$, when the friction is a reactive one (F_f^-) and $\left|\vec{v}_a\right| < \left|\vec{v}_v\right|$ it takes place the properly plastic deformation and during $T/2-2t_1$, when $\left|\vec{v}_v\right| > \left|\vec{v}_a\right|$ and the friction is positive (F_f^+), – it takes place, mostly, the metal elastic deformation / the reduction of the metal-tool contact friction, Fig.1. The vibratory rate (v_v) of the material point „P" will be obtained by the time derivative of the moving, relation (1):

$$v_v = \frac{du}{dt} = \omega \cdot A \cdot \cos\left(\frac{2\pi}{\lambda}x - \omega t\right), \tag{1}$$

The maximum value of the vibratory rate will be obtained when $\cos\left(\frac{2\pi}{\lambda}x - \omega t\right) = 1$, using the relation (2):

$$\bar{v}_v = \omega \cdot A = 2\pi \cdot f \cdot A, \tag{2}$$

where: $u = A \cdot \sin\left(\frac{2\pi}{\lambda}x - \omega t\right)$; f – vibratory frequency of the ultrasound oscillation; A – oscillation amplitude, ($\bar{A}$ – maximum of the wave oscillation – in antinodes); ω – angular frequency, ($\omega = 2\pi f$).

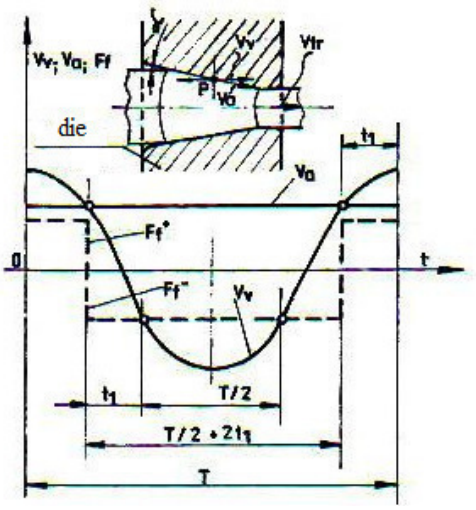

Fig. 1 – Severdenko's model about the reduction of the mean friction at the metal – tool contact surface in the technology of the metals with full section (wires, bars) drawing, (Severdenko, *et al.,* 1990): P – certain arbitrarily point placed at the metal – tool contact surface; α – half-angle of the die cone; v_a – slip rate / moving of the metal in the deformation area; v_{tr} – rate of drawing; v_v – vibratory rate of the die; F_f^- - reactive friction; F_f^+ - positive friction; T – oscillation time.

Assuming the Severdenko's model for the developing of the metal-tool contact mean friction reduction, the ratio, (Severdenko, *et al.,* 1990), given by the relation (3):

$$\varphi = \frac{(T/2 + 2t_1) + (T/2 - 2t_1)}{(T/2 + 2t_1) + (T/2 - 2t_1)}, \tag{3}$$

represents the rate of the mean friction reduction, in the considered point "P".

Because, in the technological drawing processes, the angle α has values between 8 …10°, ($\cos\alpha \rightarrow 1$; cos 8° = 0.990 and cos 10° = 0.984), it can consider that $v_a \sim v_{tr}$.

Considering $v_{tr} = v_v$, it results the relation (4):

$$t_1 = \frac{1}{\omega} \cdot \arccos \frac{v_{tr}}{v_v \cdot \cos\beta}, \tag{4}$$

The values for t_1 and T (T=1/f) will be replaced in relation (3) and it results, relation (5):

$$\varphi = \frac{\pi}{2} \cdot \frac{1}{\arccos \dfrac{v_{tr}}{v_v \cdot \cos\beta}}, \tag{5}$$

Considering that the rate of drawing has the mean value (based on the continuity equation of the metal flow), for the input-output sections in the plastic deformation focus area, the rate of the mean friction reduction (φ

coefficient), on the entire metal-tool contact area, is given by the relation (6):

$$\varphi = \frac{\pi}{2} : \arccos \frac{v_{tr} \cdot \frac{\lambda_i \cdot \cos\alpha + 1}{2\lambda_i \cdot \cos\alpha}}{\bar{v}_v \cdot \cos\beta}, \tag{6}$$

or, the estimative value of this coefficient is given by the relation (7):

$$\varphi = \frac{\pi}{2} \cdot \frac{\bar{v}_v}{v_{tr}} \cdot \frac{2\lambda_i \cdot \cos\alpha}{\lambda_i \cdot \cos\alpha + 1} \cdot \cos\beta, \tag{7}$$

For cos β = 1, it results β = 0°, so, it means that the maximum efficiency will be obtained when the drawing tool is ultrasound activated along the drawing direction.

In relations (6) and (7), λ_i represents the elongation. Because our researches were made with the tubes drawing by using one single dye, $\lambda_i=\lambda_1=S_0/S_1$, ($S_0=\pi(R_0^2 - r_0^2)$, $S_1= \pi(R_1^2 - r_1^2)$ and $\lambda_1=1{,}18$. The rate of the section reduction can be determined using the relation, (Susan, 2008; Gavrilă, 2010): $\delta=100[1-(R_1/R_0)^2] = 19\%$. The determining of the drawing force with and without ultrasounds, (F^{UVD} and F^{CT}) is made with the loading cell ΔT – 106.00 and with the tensometrical bridge N 2314. The relative reduction of the drawing force or the technological efficiency – UVD is given by the relation (8), (Susan, 2008; Gavrilă, 2010):

$$\Delta F = \frac{F^{CT} - F^{UVD}}{F^{CT}} \cdot 100[\%], \tag{8}$$

2. Material and the Research Methodology

2.1. Researched Material

For the researches, there were used tubes made from stainless steel 10TiNiCr180/AISI 321, manufactured by S.C. OMEGATUB S.A. Iasi, which had the following dimensions: D_0=5,50mm, g_0=0,70mm and l_0=1200mm; one of the ends was processed by cold rolling and thermal treated by solution quenching.

The tubes, made from stainless steel, are manufactured using a classical rolling technology, from sheet-metal strips, figured through more than one rolling-mill stands and then welded along the generating line by WIG proceeding. The chemical composition of the stainless steel 10TiNiCr180 type, spectrographycal determined is presented in Table 1.

Table 1
Chemical Composition of the Stainless Steel 10TiNiCr180 type, [%]

C	Mn	Si	Cr	S	P	Ti	Ni
0,02	1.40	0.5	19.40	0.06	0.05	0.7	10,8

The microscopic structure of the cold plastic deformed steel is made from austenite polyhedron crystals-twin crystals with discrete ferrite separations at the crystals borders.

2.2. Research Methodology

The objective of the experimental study is to give a characterization of the tubes drawing through convergent conical dies, ultrasonic activated along the drawing direction/UVD system in comparison with the classic drawing technology/CT (without ultrasound activated of the die).

There were used dies with cores from metallic carbides, (WCr), made by S.C. Industria Sarmei S.A./S.C. Mechel S.A., with the cone half-angle α=8°.

The tubes drawing was realized on the longitudinal drawing bench/12tf belonging to S.C. Rezistoterm S.R.L. Iasi; it was used the chlorided paraffine as lubricant. The oscillator system used in the research is presented in Fig. 2.

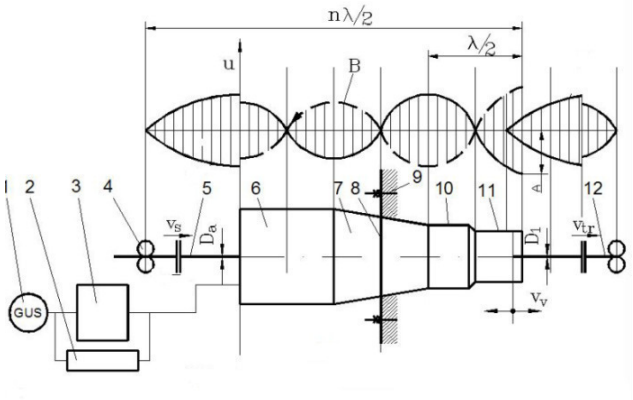

Fig. 2 – Scheme of the oscillator system used in the researching process, (Gavrilă, 2010): *a* – wave oscillation; *b* – properly scheme: 1 – ultrasonic generator, 2000W, f = 17500Hz; 2, 3 – polarization block; 4, 12 – ultrasonic energy reflectors; 5 – tube semi - product; 6 – magnetostrictor transducer; 7 – conic concentrator; 8 – noduled flange; 9 – resistance structure / frame of drawing equipment; 10 – graded cylindrical concentrator; 11 – draw-plate; 12 – drawn tube; v_{tr} – rate of drawing; v_v – vibratory rate of the die; v_s – slip rate; λ – wave length; D_a – diameter of the semi-product tube; D_1 – diameter of the processed tube; A – oscillation amplitude (vibration) of the draw-plate; —— running wave; ------ regressive wave.

3. Influence of the Rate of Drawing, (v_{tr})

The rate of drawing is a very important parameter of the stainless steel tubes drawing technology because it gives information about the efficiency of the drawing process. The rate of drawing, usually used in the classical technology, (CT), of the tubes drawing by S.C. Rezistoterm S.R.L. has the following values: 4, 6, 8 and maximum 10m/min, (0,06; 0,10; 0,13 and 0,16 m/s).

The value of the coefficient of the mean friction reduction, (φ), can be determined using the relation (6) and it is a function depending on the ratio v_{tr}/v_v with $\beta=0^{\circ}$. So, using the calculation algorithm presented in Fig. 4, there were drawn the variation curves $\varphi=f(v_{tr})$ for three values of the die oscillation amplitude, (A=25; 20 and 15μm), respectively for v_v=2,74; 2,19 and 1,64m/s, Fig. 3, (Gavrilă, 2010).

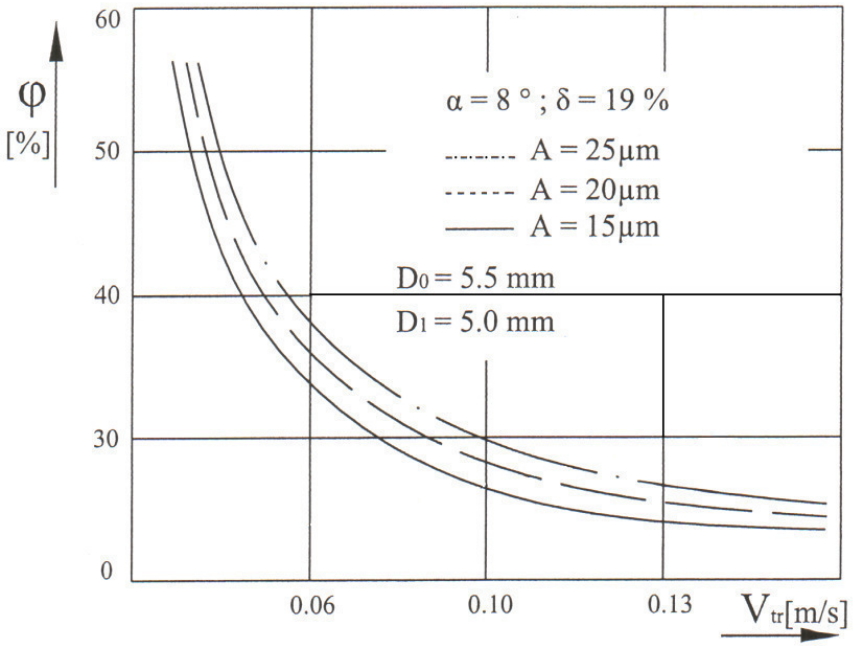

Fig. 3 – Variation of the coefficient φ depending on the rate of drawing v_{tr}.

The reduction of the metal-tool contact friction during the stainless steel tubes drawing in UVD system goes to the decreasing of the total force of drawing.

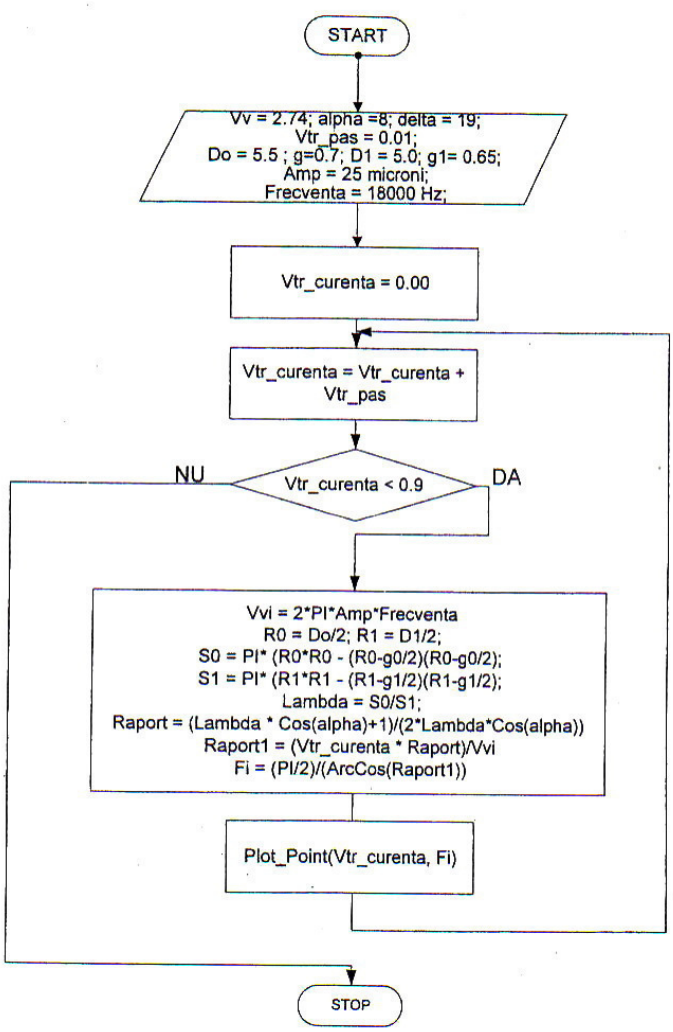

Fig. 4 – Calculation and graphical drawing algorithm of the coefficient φ variation, as a rate of drawing, v_{tr} function.

The experimental results about the influence of the rate of drawing up to the total force of drawing, obtained by S.C. Rezistoterm S.R.L. in the 10TiNiCr180 stainless steel tubes processed without inside guard drawing technology, are presented in Table 2 and Fig. 5.

The tubes processing in ultrasound field it will be realized in the next conditions: f=17.500 Hz and A=25 μm. Assuming the relation (2) it result v_v=2,74 m/s.

The relative reduction of the rate of drawing, ΔF[%], can be determined based on the relation (8). The graphical variation of the force of drawing in

UVD Technology, F^{UVD}, and of the relative reduction of the rate of drawing, ΔF[%] can be observed in Fig. 5 and 6.

Table2

Influence of the Rate of Drawing up to the Total force of Drawing, in the 10TiNiCr180 Stainless Steel Tubes Drawing Technology

Nr. crt.	Parameters of the drawing process						Force parameters			
	D_0 [mm]	g_0 [mm]	D_1 [mm]	g_1 [mm]	α [^{0}]	v_{tr} [m/s]	δ [%]	F^{TC}	F^{UVD}	ΔF [%]
1	5.50	0.70	5.0	0.65	8	0.06	19	1332	940	29.42
2	5.50	0.70	5.0	0.65	8	0.10	19	1332	986	25.97
3	5.50	0.70	5.0	0.65	8	0.13	19	1332	1052	21.02
4	5.50	0.70	5.0	0.65	8	0.16	19	1332	1106	16.96

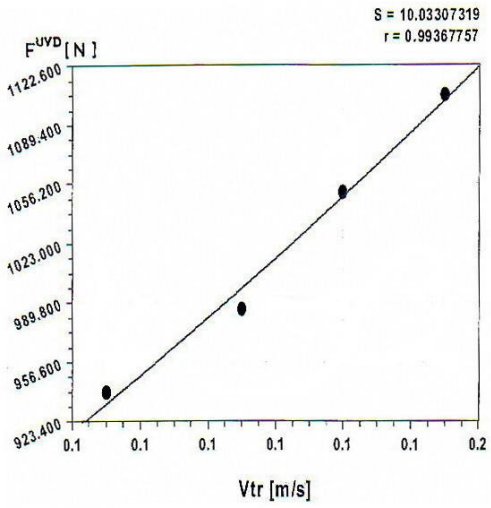

Fig. 5 – Graphical variation F^{UVD} as a function of the rate of drawing.

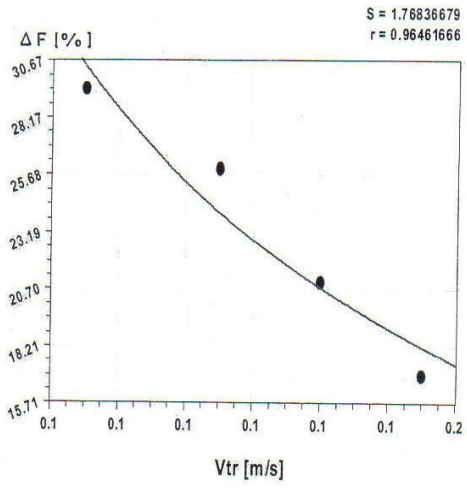

Fig. 6 – Graphical variation $\Delta F = f(v_{tr})$.

4. Conclusions

The paper presents the influence of the rate of drawing up to the total force of drawing, for the 10TiNiCr180 stainless steel tubes which were without inside guard drawn in ultrasound field/UVD Technology, when the die is placed in the antinodes of the wave oscillations and it is activated along the drawing direction and when, at the metal-tool contact surface, "the ultrasounds surface effect" or "the reduction of the metal-tool contact friction effect" takes place.

Assuming the Severdenko's model, the reduction rate of the metal-tool contact friction is given by the coefficient φ, relation (6), as a ratio v_{tr}/v_v

function. When v_v is a constant, the greater efficiency of the new technology (ΔF) is, the smaller value of the rate of drawing, (v_{tr}) is. This means that the new technology is recommended for the processing of the tubes, without inside guard, and made from metallic materials which have a strong harden by cold plastic deformation. The reduction of the drawing force (ΔF) is not a direct objective but a consequence of "the ultrasounds surface effect". It can be a technological objective "the reduction of the metal-tool contact friction effect", respectively, the hardening caused by "the ultrasounds surface effect" and all the processes, as a consequence, referring at the quality of this so processed tubes.

REFERENCES

Gavrilă B.L., *Raport de cercetare.* Anul I – proiect EURODOC, 2010.

Severdenko V.P., *Prokatkia i volocenie c ulitrazvukom*. NAUKA I TEHNICA, Minsk, 1990.

Susan M., *Deformarea metalelor prin tragere. Elemente de teoria şi tehnologia tragerii sârmelor, barelor şi ţevilor*. Ed. TEHNOPRESS, Iaşi, 2002.

Susan M., *Tragerea metaleleor cu vibraţii ultrasonice*. Edit. CERMI, Iaşi, 2008.

INFLUENŢA VITEZEI DE TRAGERE LA PROCESAREA ŢEVILOR FĂRĂ GHIDAJ INTERIOR ÎN CÂMP ULTRASONOR

(Rezumat)

Lucrarea scoate în evidenţă influenţa vitezei de tragere, (v_{tr}), la procesarea ţevilor fără ghidaj interior în câmp ultrasonor / sistem UVD, atunci când filiera este situată în maximul oscilaţiei undelor şi activată ultrasonor pe direcţia tragerii. Este cazul ţevilor procesate din materiale metalice puternic ecruisabile prin deformare plastică la rece.

BULETINUL INSTITUTULUI POLITEHNIC DIN IAŞI
Publicat de
Universitatea Tehnică „Gheorghe Asachi" din Iaşi
Tomul LVII (LXI), Fasc. 1, 2011
Secția
ŞTIINȚA ŞI INGINERIA MATERIALELOR

PULSED LASER DEPOSITION OF Ti THIN FILMS ON CAST IRON SUBSTRATE

BY

ANCA ELENA LĂRGEANU*, DAN-GELU GĂLUŞCĂ, MARICEL AGOP and MANUELA CRISTINA PERJU

"Gheorghe Asachi" Technical University of Iaşi,
Faculty of Materials Science and Engineering

Received: February 14, 2011
Accepted for publication: March 28, 2011

Abstract. In this paper is present the technique of pulsed laser deposition (PLD), who change strongly from the initial light absorption in a target to the final deposition and growth of a film. One of the primary advantages of PLD is the stoichiometric transfer of material from target to a film on a substrate. The purpose of obtaining thin films by laser ablation is to improve corrosion resistance of certain materials in machine building industry. The study is based on microscopic analysis with Ti layers deposited on iron substrate using scanning electron microscope (SEM).

Key words: pulsed laser deposition, thin layers, SEM, EDX, titanium.

1. Introduction

Laser has been developed into a powerful tool in many application. It is especially useful in material processing (Metev, *et al.,* 1994). Laser possesses have many unique properties such as narrow frequency bandwidth, coherence

*Corresponding author; *e-mail*: pufankapuf@yahoo.com

and high power density. Besides, due to its high precision, reliability and spatial resolution, it is widely used in the industry for machining of thin films, modification of materials, material surface heat treatment, welding and micro patterning.

Lasers of different types found their applicability in various fields from amusement parks to guns. Main field of engineering in witch laser is applied are (http://laserul.idilis.ro) optical communications computer and integrated optics; production and diagnostics of plasma; automatic control of cars; heating materials without phase modification; melting and welding metals; vaporizing and thin layer deposition; ultra-fast photography; testing electronic components.

Apart from these, poly-component materials can be ablated and deposited onto substrates to form stoichiometric thin films. This last mentioned application of laser is the so-called pulsed laser deposition (PLD) (Chrisey *et al.,* 1994).

Pulsed laser ablation deposition (PLD) represents an efficient and low cost method for the growth of thin films of any material (Guido *et al*., 2004).

Pulsed laser deposition (PLD) is a thin film deposition (specifically a physical vapor deposition, PVD) technique where a high power pulsed laser beam is focused inside a vacuum chamber to strike a target of the material that is to be deposited. This material is vaporized from the target (in a plasma plume) which deposits it as a thin film on a substrate (such as a silicon wafer facing the target).

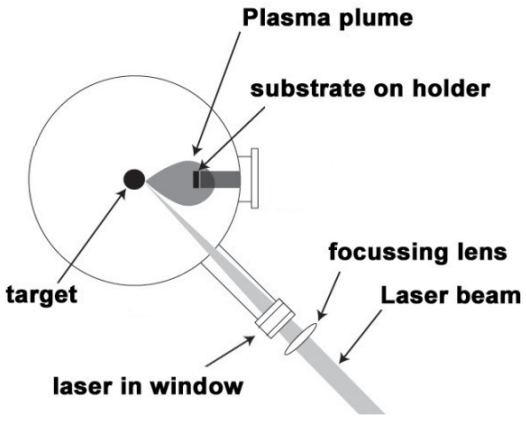

Fig. 1 – PLD deposition chamber.

This process can occur in ultra high vacuum or in the presence of a background gas, such as oxygen which is commonly used when depositing oxides to fully oxygenate the deposited films. In PLD, a large super saturation occurs on the substrate during the pulse duration. The pulse lasts around 10–40 microseconds depending on the laser parameters, (Granozio *et al.,* 2006).

2. Results and Discussions

Coating attempts using pulsed laser deposition (PLD) method and thin layers were obtained to improve corrosion resistance. For the experiment grey cast-iron was used as base material STAS 568/82, and titan as coating material.

Chemical composition of base material used is presented in Table 1 and was determined with Foundry Master Spectrometer (Lărgeanu *et al.,* 2011).

Table 1

Chemical Composition of Cast-Iron, %

Material	Fe	C	Si	Mn	P	S	Cr	Ni	Cu
Cast-iron	91.8	4.50	1.54	1.03	0.62	0.14	0.096	0.057	0.148

PLD coating method conditions were established in a manner to favor TiO developing at the surface, witch is a compound with good anti-corrosive proprieties. Coating layers were studied by electronic microscopy and EDX analysis.

In Fig. 2 electronic microscopies are presented made with a secondary electrons detector (SE) from the surface of deposited metallic material in a nano-metric titan layer using laser ablation. Microscopy's are made at 100µm, at the border between the coating layer and the base material (Fig. 2 *a*), on the coating layer (Fig. 2 *b*) and at 10 µm (Fig. 2 *c*).

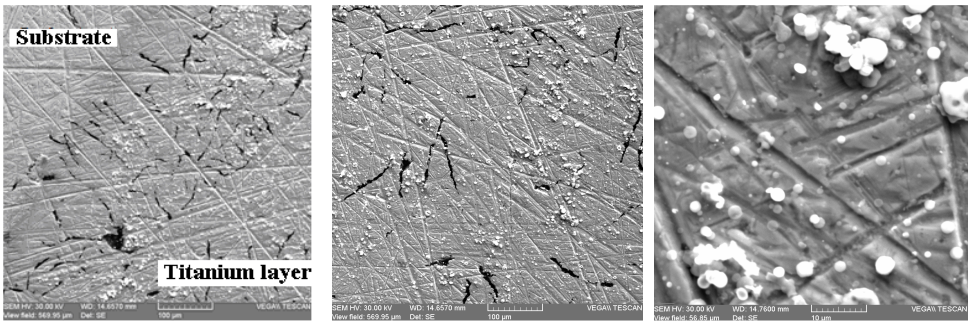

a *b* *c*

Fig. 2 – SEM micro-cracks for cast-iron sample coated with Ti nanometer layer using laser ablation: 100 µm highlighting the border between the substrate and the deposited layer (*a*), 100 µm Ti layer (*b*) and 10 µm Ti layer (*c*).

In Fig. 3 two selected points are presented, one on the sub-layer (Fig. 3 *a*) and the other on the coating layer, for witch chemical analysis will be performed with EDX.

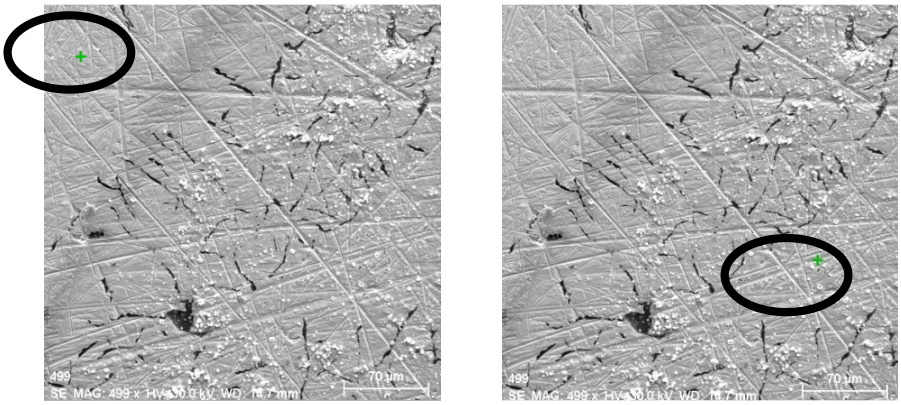

a *b*

Fig. 3 – SEM microstructures for interest areas on witch are highlighted two points: *a* –for chemical analysis; *b* – one on the sub-layer and the other on the coating layer

Chemical analysis reveals material composition in selected points with the values in Table 2 and 3. Main elements from the sub-layer are iron, carbon, silicon, manganese and phosphorus. These elements are characteristic to substrate used cast-iron with presenting the energies spectrum.

The sub-layer is a cast-iron with a high iron percentage. Mass and atomic percents of base material elements are highlighted in Table 2.

Table 2

Chemical Composition in Selected Point From Picture 3a

Element	norm. wt. [%]	norm. at. [%]	Error in [%]
Iron	94.14379	85.16814	2.290446
Carbon	2.217285	9.32669	0.484431
Silicon	1.898785	3.415693	0.124683
Manganese	1.052586	0.967988	0.101665
Phosphorus	0.687552	1.121493	0.064368

The point in which chemical composition was performed is selected in Fig. 3 *b*; is presenting an atomic percent of titanium and mass percent close to 3.5% and also a high mass percent of oxygen around 4.9% specific to TiO formations developed at the surface of the material covered with titanium by laser ablation.

Titanium and titanium oxide superficial layer obtained by laser ablation is at nanometers scale. EDX analysis made possible elements detection: iron, manganese, silicon, elements from the substrate, identified also in the material energy spectrum.

Tabel 3

Chemical Composition in Selected Point From Picture 3 b

Element	norm. wt. [%]	norm. at. [%]	Error in [%]
Iron	87.96598	73.95346	2.227107
Oxygen	4.297309	12.61062	6.963392
Titanium	3.526408	3.457977	0.130003
Silicon	1.995947	3.336649	0.129916
Carbon	1.554777	6.077607	0.369664
Manganese	0.659581	0.563688	0.092122

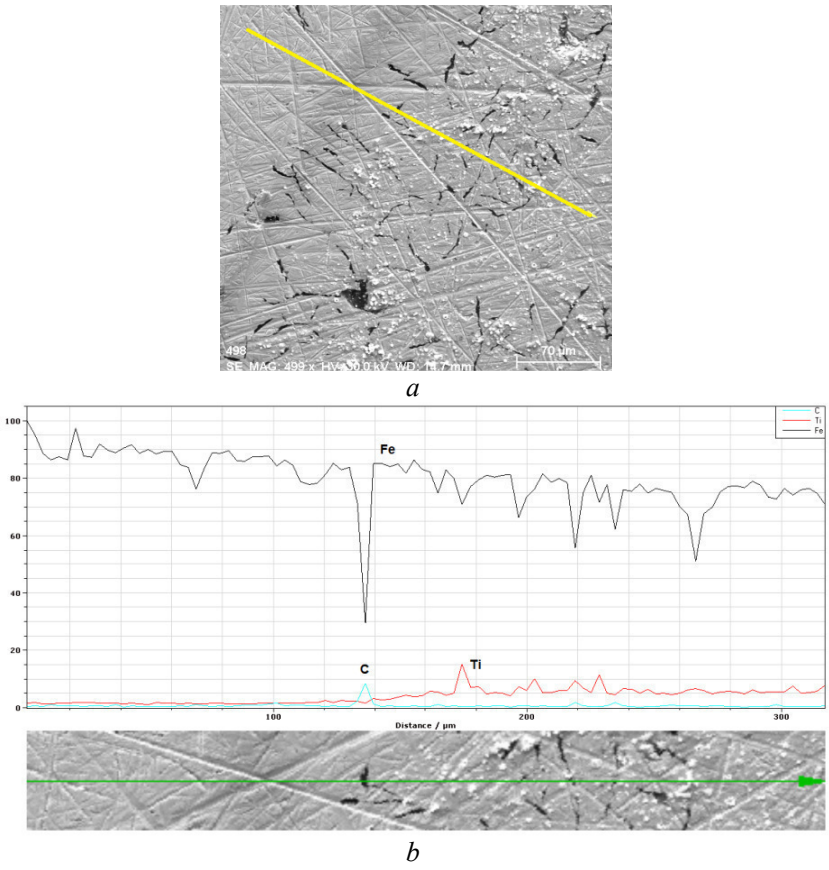

a

b

Fig. 4 – Chemical elements distribution titanium, iron and carbon on a selected line.

In Fig. 4 is presented chemical elements distribution titanium, iron, and carbon. Analyzed elements are marked on the images and are characterizing titanium distribution on the superficial layer surface obtained with laser ablation. On the right side of the distribution is highlighted the quality of

titanium element observing it's contribution around the big particles witch compose the deposited layer.

Chemical analysis for laser ablation obtained layer is continued by exemplifying the distribution of main chemical elements composing the layer and sub-layer by distribution of these elements on the interest selected area presented in picture 5 *a*. Element distribution iron, titanium and carbon are presented in picture 5 *b*.

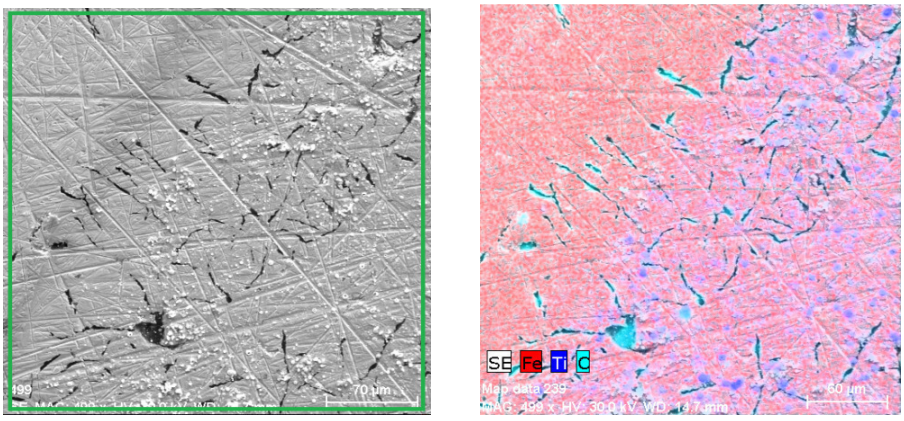

a *b*

Fig. 5 – Element distribution iron, carbon and titanium on the laser ablation deposition area: *a* – selected area, *b* – main elements distribution.

We can observe, from the analysis, a good homogeneity for the coating layer with a high compactness and the participation of titanium and titanium oxide particles of small dimensions, nanometers scale, medium 1-2 μm and large 5-6 μm.

3. Conclusions

1. Laser ablation represents a special method to grow thin layers with big advantages regarding control and develop.

2. Microscopic analysis reveal crystalline structure of obtained layers with different particles with dimensions from nanometers to micrometers depending of atoms, ions and radicals species speed emitted from the target material under laser beam action.

3. Layers obtained by laser ablation are homogeneous, of small dimensions and compact, improving the material used as sub-layer from corrosion point of view, benefiting mainly of the titanium oxide layer at the surface.

REFERENCE

[*] http://laserul.idilis.ro

Chrisey D.B., Hubler G.K., *Pulsed Laser Deposition of Thin Film*. John Wiley & Sons, Inc., New York, 1994.

Granozio F.M. *et al*., *In-situ Investigation of Surface Oxygen Vacancies in Perovskites*. Mat. Res. Soc. Proc. **967e**, (2006).

Guido D., Cultrera L., Perrone A., *The Pulsed Laser Ablation Deposition Technique: a New Deposition Configuration for the Synthesis Of Uniform Films*. Surface and Coatings Technology 180 –181, 603–606 (2004).

Lărgeanu A.E., Nejneru C., Perju M.C., Găluşcă D.G., *Thermal Conductivity Analysis for Metallic System Obtained Multiple Coating by Electro-Spark Deposition Method*. Metalurgia International, **5**, 43-46 (2011).

Metev S.M., Veiko V.P., *Laser Assisted Microtechnology*. Springer, Berlin, Heidelberg 1994.

Ursu C., *Diagnoza electrica Si optică a plasmei produsă prin ablaţie laser*. Ph. D. Diss., Iaşi, 2010.

DEPUNEREA PRIN ABLAŢIE LASER DE STRATURI SUBŢIRI DE Ti PE SUBSTRAT DE FONTĂ

(Rezumat)

In această lucrare este prezentat tehnica depunerii cu pulsaţii laser (PLD), care modifică puternic din absorbţie a luminii iniţială într-o ţintă pentru depunerea finală şi de creştere a unui film. Unul dintre avantajele principale ale PLD este transferul stoichiometric de material de la ţintă la un film pe un substrat. Scopul obţinerii straturilor subţiri prin ablaţie laser este de a îmbunătăţi rezistenţa la coroziune a unor materiale din industria construcţiilor de maşini. Studiul se bazează pe analiza microscopică a straturilor depuse cu Ti pe substrat de fontă, utilizând microscopul cu scanare de electroni (SEM).

BULETINUL INSTITUTULUI POLITEHNIC DIN IAŞI
Publicat de
Universitatea Tehnică „Gheorghe Asachi" din Iaşi
Tomul LVII (LXI), Fasc. 1, 2011
Secția
ŞTIINȚA ŞI INGINERIA MATERIALELOR

LIGHTWEIGHT MATERIALS PROPOSE FOR UPPER LIMB RECOVERY EQUIPMENT

BY

PETRONELA PARASCHIV[1*], CIPRIAN PARASCHIV[2] and NICANOR CIMPOEŞU[3]

"Gheorghe Asachi" Technical University of Iaşi,
[1] Faculty of Hydrotechnical Engineering, Geodesy and Environmental Engineering
[2]Grigore T. Popa University of Medicine and Pharmacy
[3] Faculty of Materials Science and Engineering

Received: February 14, 2011
Accepted for publication: March 28, 2011

Abstract. Robotic recovery systems involve usage of different materials as actuation elements, fixed structure elements, platform or other that participate at the final equipment weight. An Al-Si alloy is proposed as based material for rehabilitation equipments and analyzes by thermal and microstructural behavior point of view through dilatometer and optical microscopy techniques. Both thermal and microstructural analyses reveal a good metallic material stabilization.

Key words: upper limb recovery, lightweight materials, aluminum based alloy.

1. Introduction

The field of stroke rehabilitation is changing and improving rapidly based on the electronically equipments evolution. One major recent change in

*Corresponding author; *e-mail*: nicanornick@yahoo.com

clinic recovery especially of upper and inferior limbs is the increasing availability of robotic applications for rehabilitation.

Clinicians hear about robotic applications from articles in clinical journals, vendors anxious to sell products, news coverage of amazing recoveries attributed to a new device, with more expected results by patients searching for a miracle cure, and other rehabilitation professionals.

Rehabilitation processes seeks to develop strategies compensatory as well as to induce neural plasticity and recovery. Robotics is a tool that can be used for both these goals— to assist and for individual in activities of daily living or to assess and provide therapy for that individual. This article is a critical review of the clinically relevant literature that addresses robotic applications in the assessment and treatment of post-stroke upper limb motor dysfunction.

A variety of neuro-rehabilitation strategies have been used in the design of systems for robotic rehabilitation. For instance, repetitive movement training, or massed practice, and explicit learning paradigms are used by most current robotic systems for therapy. Robotic rehabilitation protocols incorporating neuro-rehabilitation strategies such as bilateral training, implicit training, feedback distortion, and functional task paradigms are in development at this time.

It is important to incorporate motor learning principles into the design of any rehabilitation program and to consider new metallic materials for fixed parts with lightweight properties to improve the dispositive control, utilization and effect. Although there is a body of literature regarding motor learning principles in individuals without neurological impairment, little research has been conducted to determine the materials properties that can help and optimize the post-stroke motor recovery.

Most existing rehabilitation robots use a massed practice approach and an explicit learning paradigm, specifically a target endpoint or path shaping task; these assumptions being largely based on research conducted with the MIT-Manus robot demonstrating that repetitive, goal-directed, robot-assisted therapy can improve clinical outcomes (Aisen *et al.,* 1997; Volpe *et al.,* 1999; Volpe *et al.,* 2000; Krebs *et al.,* 2000).

As pointed out in different reviews (Krakauer *et al.,* 2005; Krakauer 2006) few rehabilitation robots designed for post-stroke rehabilitation make use of other motor learning strategies, despite research suggesting that alternate paradigms induce better post-stroke rehabilitation outcomes.

It has been found that implicit learning paradigms may result in greater learning effects than explicit models (Pohl *et al.,* 2006; Patton *et al.,* 2004). Implicit learning refers to skill acquisition without awareness or not directed on a conscious level; this is in contrast to explicit learning that refers to skill acquisition that is self or other directed (Cleeremans, 2003). To give

an example the implicit learning way may be incorporated into a robotic rehabilitation program by programming the target training movements into a game or other such virtual environment that the patient may explore. Other researchers found that action observation and imitation (Buccino *et al.,* 2006) and contextual interference (Hanlon, 1996) may enhance retention of post-stroke training.

The literature concerning action observation and imitation shows that robotic applications would be most successful if learning goals were demonstrated to patients first. It has been suggested that amplifying movement errors generated by patients while they train may result in greater rehabilitation gains than the more common strategy of assisting patients to move in the correct direction (Patton *et al.,* 2006). So in this manner one error magnification paradigm induces a patient's limb to actively move in a particular trajectory by perturbing the limb in the direction opposite that of the desired trajectory. The subject counters the perturbing force in order to move in a straight line the affected member. Then, when the perturbing force is unexpectedly removed, the subject will move along the desired trajectory, this procedure is known as a neuromuscular after-effect. In one clinical study involving a group of persons 7 out of 10 individuals with post-stroke hemi-paresis who were tested demonstrated retention of such corrections for at least two hours after experiencing error magnified attempts (Patton *et al.,* 2006).

A lightweight material based on aluminum and silicon chemical elements is propose for upper limb recovery system as structural fixed elements and analyzed by thermal and microstructural properties point of view.

2. Experimental Details and Results

Aluminum based alloys are considered a proper solution in medical rehabilitation process especially for upper limb member pointing the influence of the system mass and weight. An Al-Si based alloy, with chemical composition presented in Fig. 1, is propose for active support elements of the equipment to reduce the weight and for very good material properties. In this study the material behavior at heating, through dilatometer procedure, analysis and microstructure investigation by optical means were realized. For thermal investigation was used a Linseis 75 dilatometer using a 5 K/min heating rate from room temperature (RT) to 250°C.

First the material was chemical analyzed using a mass spectrometer type Fouundry-Master with aluminum and silicon bases. Reduce percentages of iron, copper and zinc is also in the alloy composition most of them by melting process and by the elements used to obtain the alloy but with good influence of all these elements on the material properties.

Foundry-Master 01J0013 Optik 01J0013
Sample : aluminiu piesa
Alloy : AL_000 Mode :PA 2/26/2008 10:16:10 AM

	Al	Si	Fe	Cu	Mn	Mg	Zn
1	82.5	13.1	0.772	1.92	0.221	0.143	0.836
Average	**82.5**	**13.1**	**0.772**	**1.92**	**0.221**	**0.143**	**0.836**

	Cr	Ni	Ti	Be	Ca	Li	Pb
1	0.0177	0.0817	0.0309	< 0.0001	0.0031	< 0.0001	0.116
Average	**0.0177**	**0.0817**	**0.0309**	**< 0.0001**	**0.0031**	**< 0.0001**	**0.116**

	Sn	Sr	V	Na	Bi	Zr	B
1	0.0986	< 0.0001	0.0065	0.0036	< 0.0050	0.0044	0.0006
Average	**0.0986**	**< 0.0001**	**0.0065**	**0.0036**	**< 0.0050**	**0.0044**	**0.0006**

	Ga	Cd	Co	Ag
1	0.0090	0.0021	< 0.0030	0.0029
Average	**0.0090**	**0.0021**	**< 0.0030**	**0.0029**

Fig. 1 – Chemical composition of Al-Si alloy.

The sample tested at temperature variation was made form of two geometrical shapes, the main structural elements in a rehabilitation system are usually cylindrical or parallelepiped, presented in Fig. 2 to follow the material behavior under thermal conditions respecting the plan conditions.

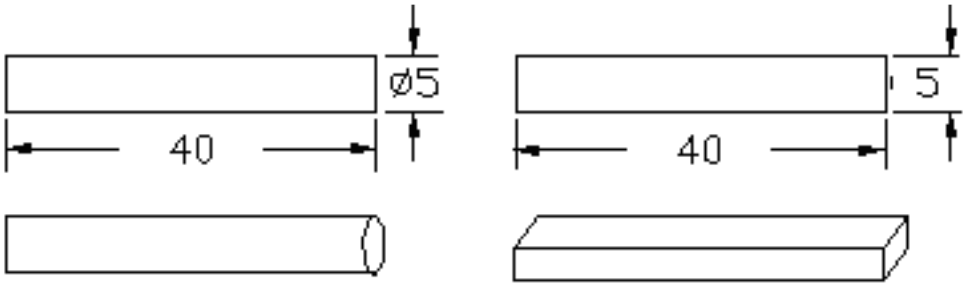

Fig. 2 – Sample sketch of the Al-Si material used in dilatation tests.

The sample experimental dimensions here 40.59 mm long and 50.6 mm width using a 5 K/min temperature rate. In table 1 inside oven and sample temperature are establish by free observation of the dilatometer equipment from 1 minute to another determining a “in situ” thermal conductivity of the material. The equipment is based on two temperature sensors that register the temperature on the sample and inside the furnace.

Table 1
Temperature Variation of a Metallic Sample and the Oven in a Dilatometric Test Realized on a Linseis Equipment

Time [min]	Sample Temperature [°C]	Oven temperature [°C]	Time [min]	Sample Temperature [°C]	Oven temperature [°C]
0	22	27	**21**	233.8	326
1	23.2	57,6	**22**	244	333
2	24.7	83,4	**23**	250	340
3	27.6	112,5	**24**	262	349
4	33.9	141,6	**25**	270	357
5	41.3	171,6	**26**	279	367
6	51.4	195,6	**27**	288	376,8
7	61.2	215,6	**28**	297	386
8	73.1	234,4	**29**	306	396
9	87.4	250	**30**	317	405
10	100.2	262	**31**	326	414
11	118.5	270	**32**	337	427
12	130	279	**33**	345	431
13	144.7	285	**34**	348	435
14	164.6	295	**35**	352	436
15	174.6	300	**36**	356	426
16	188.4	305,3	**37**	361	409
17	192.7	308	**38**	**367**	**367**
18	201.6	310	**39**	358	341
19	216.8	315	**40**	343	320
20	226	321	**41**	332	301

The thermal variations exhibit a reduce transfer of heat at the beginning with more than 140°C differences between the oven temperature and the sample fact that create a thermal inertia of the sample temperature reaching a maximum 367°C temperature that was not propose for the experiment having no research interest in this field of applications. The equipment function is based on reaching a propose temperature of the sample and paying respect for his properties the oven temperature must increase less or more to achieve that goal.

In Fig. 3 are presented the oven and sample temperatures variation in time including a cooling domain. The metallic material behave classic with no internal state modifications facts that increase the thermal stability properties of these cheap to prepare materials that can be used as connection elements in any lightweight structure. Having a thermal behavior characterization of a metallic material this can be easily controlled in any structural activity at any room or environment temperature.

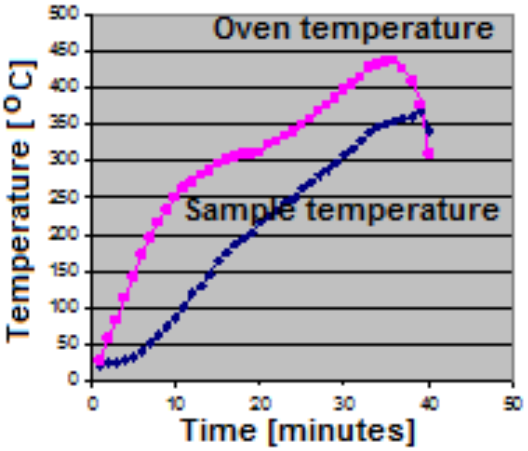

Fig. 3 – Heating of Al-Si alloy graph.

In Fig. 4 a dilatometer result is presented concerning the dimensional variation of an Al-Si alloy during a thermal variation process. Dimensional the material behaves very small modifications especially in 22 to 75ºC temperature range with values between 0.5 and 1.5 µm. for higher temperatures the Al-Si alloy dilatation increase reaching a 180.3 µm value.

The material microstructure after mechanical working operations like debiting, forging, heat treatment apply on the material for a finite element obtaining is presented in Fig. 5. Microstructure was reveal through optical microscopy after mechanical brazing of the material and a Regal water solution chemical attack.

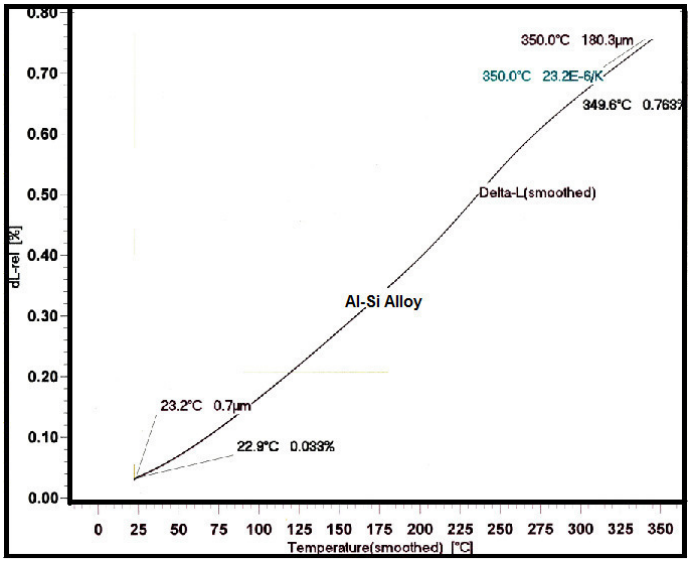

Fig. 4 – Dilatometer result on a Al-Si alloy.

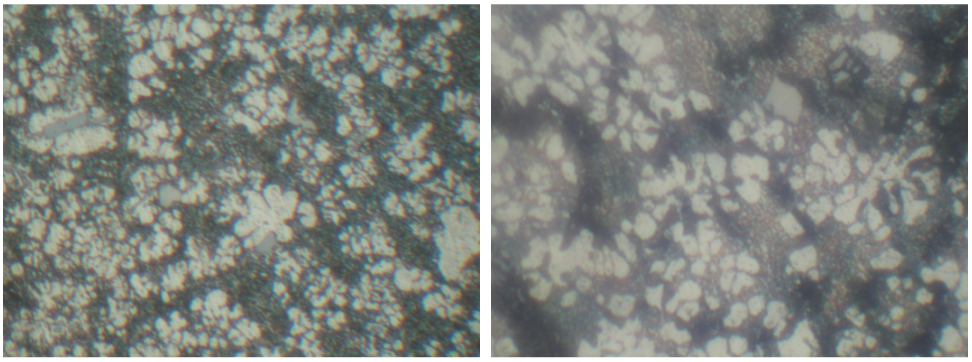

a *b*

Fig. 5 – Optical microstructure images of Al-Si alloy in: *a* – middle sample area and *b* – border sample area for a 500x image amplification.

The microstructural analyze was realized in the middle of the final prepared piece and on the border to compare eventual modifications of the sample. The microstructure are similar and characterize the microstructural stability of the propose material after different mechanical working operations.

3. Conclusions

Robotic rehabilitation systems gain more and more space on clinical procedures for recovery actions of different human body parts and an important aspect is the system weight. A lightweight material based on aluminum with great corrosion resistance, nice thermal properties and microstructural stability after different processing operations is propose to be used as fixed elements in recovery equipments.

REFERENCES

Aisen M.L., Krebs H.I., Hogan N., McDowell F., Volpe B.T., *The Effect of Robot-Assisted Therapy and Reha-Bilitative Training on Motor Recovery Following Stroke*. Arch Neurol., **54**, 443–446 (1997).

Buccino G., Solodkin A., Small S.L., *Functions of the Mirror Neuron System: Implications for Neurorehabilitation*. Cogn Behav Neurol., **19**, 55–63 (2006).

Cleeremans A., *Implicit Learning. In: Nadel L, ed. Encyclopedia of Cognitive Science.* London: Nature Publishing Group, 2003.

Hanlon R.E., *Motor Learning Following Unilateral Stroke*. Arch. Phys. Med. Rehabil., **77**, 811–815 (1996).

Krakauer J.W., *Arm Function after Stroke: from Physiology to Recovery*. Semin. Neurol., **25**, 384–395 (2005).

Krakauer J.W., Motor *Learning: it's Relevance to Stroke Recovery and Neurorehabilitation*. Curr Opin Neurol., **19**, 84–90 (2006).

Krebs H.I., Volpe B.T., Aisen M.L., Hogan N., *Increasing Productivity and Quality of Care: Robot-Aided Neuro-Rehabilitation.* J. Rehabil Res. Dev., **37**, 639–652 (2000).

Patton J.L., Stoykov M.E., Kovic M., Mussa-Ivaldi F.A., *Evaluation of Robotic Training Forces that Either Enhance or Reduce Error in Chronic Hemiparetic Stroke Survivors.* Exp. Brain. Res., **168**, 368–383 (2006).

Patton J.L., Kovic M., Mussa-Ivaldi F.A., *Custom Designed Haptic Training for Restoring Reaching Ability to Individuals with Poststroke Hemiparesis*. J Rehabil Res. Dev., **43**, 643–656 (2006).

Patton J.L., Mussa-Ivaldi F.A., *Robot-Assisted Adaptive Training: Custom Force Fields for Teaching Movement Patterns.* IEEE Trans. Biomed. Eng., **51**, 636–646 (2004).

Pohl P.S., McDowd J.M., Filion D., Richards L.G., Stiers W., *Implicit Learning of a Motor Skill after Mild and Moderate Stroke.* Clin Rehabil., **20**, 246–253 (2006).

Volpe B.T., Krebs H.I., Hogan N., Edelstein O.L., Diels C., Aisen M., *A Novel Approach to Stroke Rehabilita- Tion: Robot-Aided Sensorimotor Stimulation.* Neu- Rology., **54**, 1938–1944 (2000).

Volpe B.T., Krebs H.I., Hogan N., Edelsteinn L., Diels C.M., Aisen M.L., *Robot Training Enhanced Motor Outcome in Patients with Stroke Maintained Over 3 Years.* Neurology., **53**, 1874–1876 (1999).

MATERIALE UŞOARE PROPUSE PENTRU REALIZAREA UNUI ECHIPAMENT DE REFACERE A MEMBRULUI SUPERIOR

(Rezumat)

Sistemele de recuperare robotice implică utilizarea a diferite materiale sub formă de elemente de actuație, platforme de susținere, elemente structural fixe sau alte elemente ce contribuie împreună la greutatea finală a echipamentului. Un aliaj pe bază de Al-Si este propus pentru realizarea elementelor principale ale echipamentelor de reabilitare şi analizat din punct de vedere al comportamentului termic şi microstructural prin tehnici de analiză de dilatometrie şi microscopie optică. Atât analizele termice cât şi cele microstructurale prezintă o stabilitate foarte bună a materialului metalic.

BULETINUL INSTITUTULUI POLITEHNIC DIN IAŞI
Publicat de
Universitatea Tehnică „Gheorghe Asachi" din Iaşi
Tomul LVII (LXI), Fasc. 1, 2011
Secția
ŞTIINȚA ŞI INGINERIA MATERIALELOR

OBTAINMENT OF Fe-Mn-Si-Cr-Ni SMAs BY POWDER METALLURGY

BY

BOGDAN PRICOP*, NICOLETA MONICA LOHAN and LEANDRU-GHEORGHE BUJOREANU

"Gheorghe Asachi" Technical University of Iaşi,
Faculty of Materials Science and Engineering

Received: February 14, 2011
Accepted for publication: March 28, 2011

Abstract. By means of scanning electron microscope (SEM) and x-ray diffraction (XRD) the texture evolution and microstructural changes of a Fe-14Mn-6Si-9Cr-5Ni (%) powder was observed. After sintering the powder, the samples obtained were hot rolled at 1370 K followed by XRD measurement to identify the presence of ε martensite. The samples were ring formed and tested for shape memory effect (SME) varying the applied temperature.

Key words: Fe-Mn-Si-Cr-Ni, shape memory alloy, scanning electron microscopy, X-ray diffraction, powders.

1. Introduction

Fe-Mn-Si-Cr-Ni alloys produced by classical metallurgy based on melting, alloying and casting present several technological drawbacks such as: compositional segregation, difficult incorporation of Si into melt, manganese loss on melting and heat treatment, time consuming chemical composition homogenization, cooling contraction during solidification and quenching, tempering embrittlement, etc. (Berns *et al.,* 2008).

*Corresponding author; *e-mail*: pricopbogdan@ymail.com

A solution to avoid most of these problems could be powder metallurgy (PM) which has been successfully applied to other SMAs such as Ti-Ni or to Cu base alloys (Suzuki *et al.,* 1998). Assuming that most of the difficulties in preparing grain refined microstructures of Fe-Mn-Si-Cr-Ni SMAs with homogenous structure can be eliminated by mechanical alloying (MA) (He *et al.,* 2006), it is expected that one of its effects on PM Fe-Mn-Si-Cr-Ni SMAs would consist in increasing the solid-state solubility of alloying elements into Fe matrix (Hightower *et al.,*1997).

The Fe based SMAs have a good workability and reasonable low cost of production. The alloys are suitable for constrained recovery applications (Proft *et al.,* 1990), such as pipe joints (Kajiwara *et al.,* 2003) and rail couplings (Sato *et al.,* 2006). Considering the applications the present authors developed a Fe based SMA with the nominal composition Fe-14Mn-6Si-9Cr-5Ni to be used for pipe joints.

2. Experimental Procedure

Powder mixtures with nominal composition Fe-14Mn-6Si-9Cr-4Ni were prepared in tubular blender under protective atmosphere, from commercial powders. The obtained powders were then pressed and sintered at 1390 K, under cracked ammonia (75 % N_2 + 25 % H_2) followed by hot rolling at 1370 K (Pricop *et al.,* 2010).

The obtained specimens were analyzed by optical microscopy (OM), X-ray diffraction (XRD) and scanning electron microscopy (SEM). The optical micrographs were obtained with a MEIJI TECHNO IM7200 microscope that features an Evolution VF cooled color camera. XRD patterns were recorded on a BRUKER AXS D8 Advance diffractometer with Cu Kα and EVA software. SEM observations were done on a SEM – VEGA II LSH TESCAN scanning electron microscope, coupled with an EDX – QUANTAX QX2 ROENTEC detector and on a FEI Quanta 200 3D dual beam device.

For optical microscopy, the specimens were carefully grounded and polished and then etched with acetic glyceregia (1 ml HCl + 10 ml acid acetic + 5 ml HNO_3 + 2 drops of glycerin).

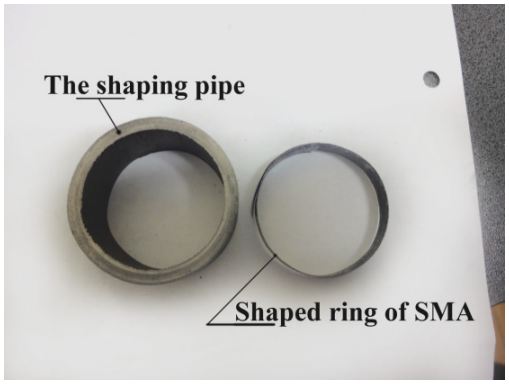

Fig. 1 – The shape setting device used for ring forming.

The hot shape imprinted to the hot rolled samples was obtained with a sectioned pipe with the same diameter as the pipes that will be joined, Fig. 1.

3. Results and Discussion

Typical aspects of as blended Fe-Mn-Si-Cr-Ni powders are presented in Fig. 2. It can be observed from Fig. 2 *a* that the Si particles, the big grey grains, are relatively big in size as compared to the other particle, meaning that the these particles were not very well milled. Fig. 2 *b* presents a few grain measurements with the average size of grains 58 μm.

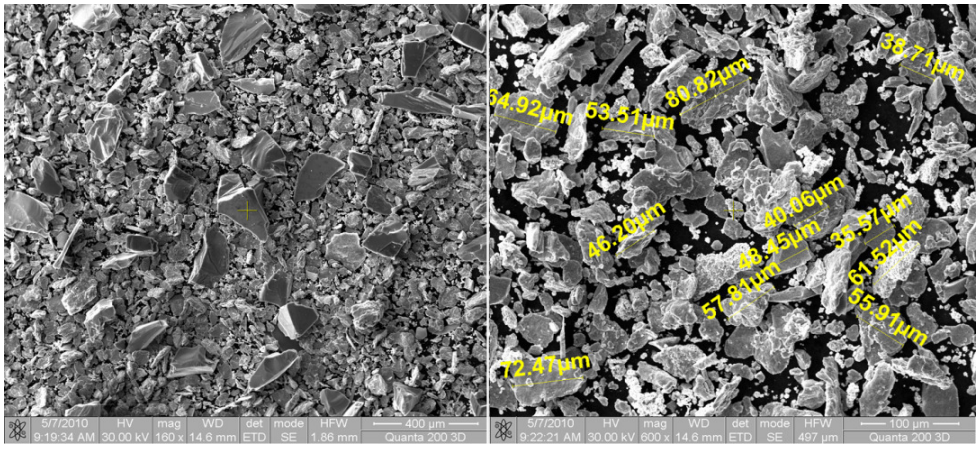

a *b*

Fig. 2 – SEM micrographs of Fe-14Mn-6Si-9Cr-5Ni (%) powder: *a* – representative micrograph; *b* – detail with grain measurement.

The XRD patterns of the obtained powders listed in Fig. 3 presents the diffraction maxima of the constituent elements.

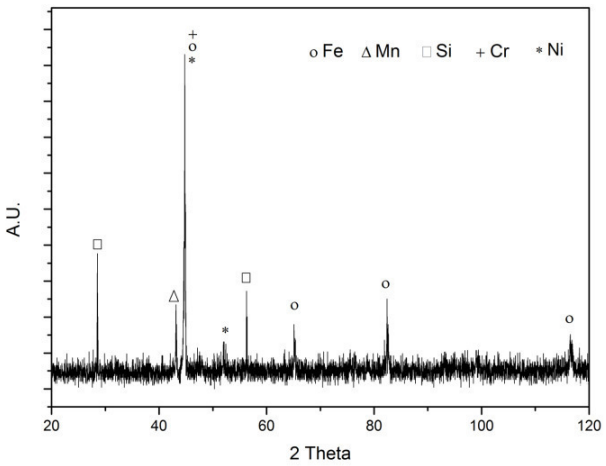

Fig. 3 – XRD patterns of Fe-14Mn-6Si-9Cr-5Ni (%) powder with element identification.

After sintering and hot rolling a sample was prepared for optical microscopy. Its typical aspect is presented in Fig. 4.

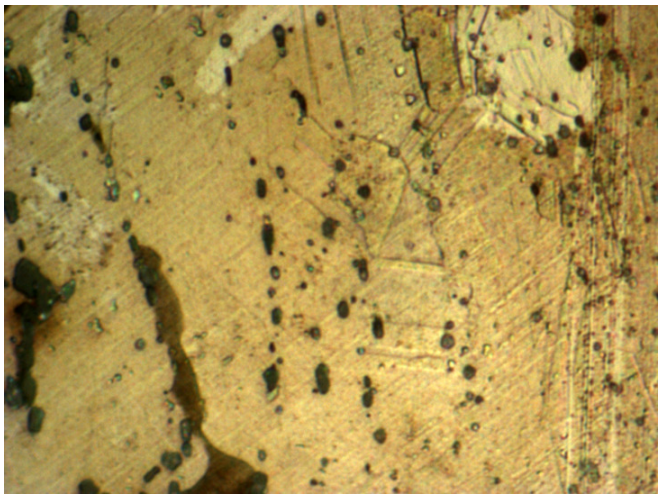

Fig. 4 – Optical micrograph of Fe-14Mn-6Si-9Cr-5Ni (%) hot rolled sample.

The general aspect of the sample consists in twins and dislocations situated throughout the surface. As an effect of applying solid solution heat treatment obvious structural changes were noticed as a function of maintaining temperature. These effects are illustrated in Fig. 5 by means of XRD patterns.

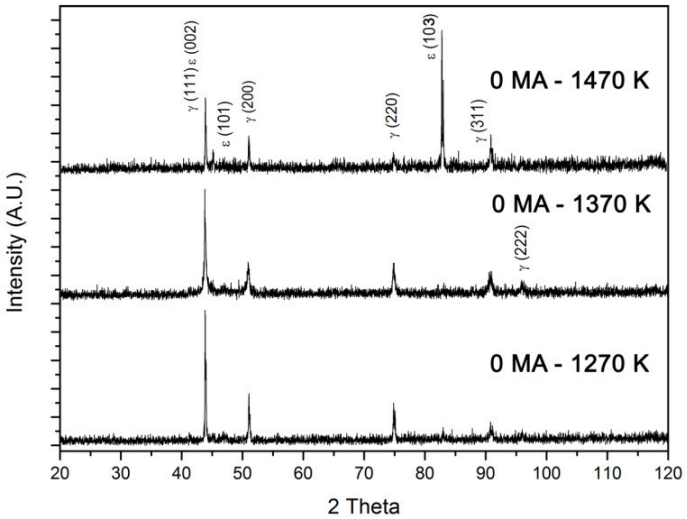

Fig. 5 – XRD patterns of the hot rolled samples that were subjected to three solution treatment temperatures, 1270 K, 1370 K and 1470 K.

The solution treated sample at 1270 K contains a large amount of austenite, γ phase, on the planes (111), (200), (220) and (311) and only small amount of ε martensite. With temperature increasing at 1370 K new austenite maxima appeared on the chart on (222) plane. Increasing furthermore the temperature at 1470 K the amount of γ phase diminished and another maxima appeared at (103) plane that was attributed to ε phase. So far the solution treatment at 1470 K produced the highest quantity of martensite and for that reason the further samples will undergo the same solution treatment temperature.

The samples were next ring formed with the device presented in Fig. 1 and subjected to a series of heating cycles in order to determine the EMF of the alloy, as shown in Fig. 6.

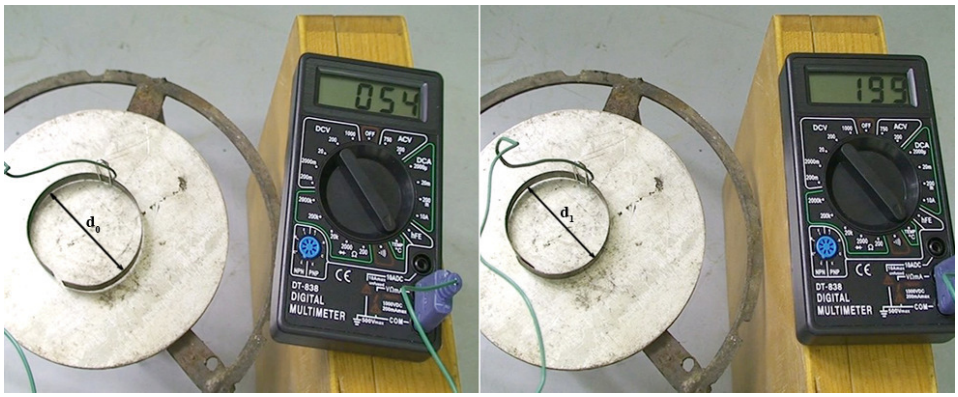

a *b*

Fig. 6 – Illustration of EMF on Fe-14Mn-6Si-9Cr-5Ni (%) ring shaped sample: *a* – the ring at the beginning and *b* – at the end of heating.

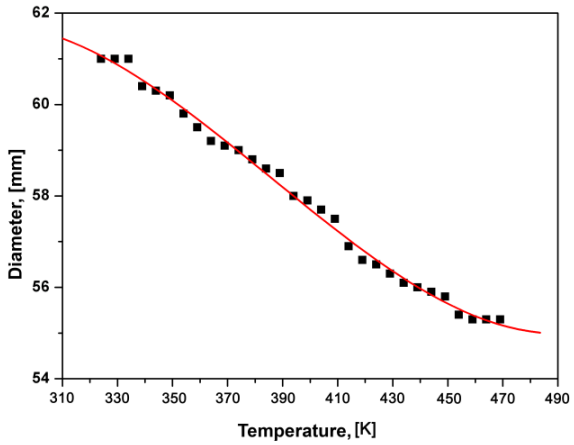

Fig. 7 – Variation of ring shaped sample inner diameter in regard to temperature.

The inner diameter of the shaped ring started from 61.4 mm and ended at 55 mm at the end of the heating cycle as presented in Fig. 7, this clearly shows that with a 10,42% reduction the ring is capable of joining two pipes together.

4. Conclusion

Commercial powders with nominal composition Fe-14Mn-6Si-9Cr-5Ni(%) were investigated. After pressing and sintering under cracked ammonia at 1390 K, followed by hot rolling at 1470 K the samples were investigated from the point of XRD and SEM. SME was tested with the ring shaped samples by heating cycles.

After the investigations were complete the following conclusion were drawn:

- from the XRD and SEM investigation appeared that the powder had a homogenous composition;
- after solution treatment at different temperature a conclusion was made that the use of 1470 K temperature was more favorable than the other temperature used, by applying it we have obtained a large quantity of ε martensite.
- the test on SME was conclusive, we've obtained a 10,42% contraction and therefore the ring can support the pipe coupling.

Acknowledgements. This paper was realized with the support of EURODOC "Doctoral Scholarships for research performance at European level" Project, financed by the European Social Found and Romanian Government.

REFERENCES

Berns H., Theisen W., *Ferrous Materials*. Steel and Cast Iron, Springer, 190-198, 378-380, 397-399 (2008).

He Q., Jia C., J. Meng, Mat. Sci. Eng. A, 428 314 (2006).

Hightower A., Fultz B., Bowman R.C.Jr., J. Alloy Compd. 252 238 (1997).

Kajiwara S., Baruj A., Kikuchi T., Shinya N., Proc. SPIE 5053 (2003) 250.

Pricop B., Söyler U., Comaneci R.I., Özkal B., Bujoreanu L.G., Physics Procedia, **10,** 125–131 (2010).

Proft J.L., Duerig T.W., in: T.W. Duerig, K.N. Melton, D. Stöckel, C.M. Wayman (Eds.), *Engineering Aspects of Shape Memory Alloys*. Butterworth Heinemann, London, 115–129 (1990).

Sato A., Kubo H., Maruyama T., Mater. Trans. **47**, 571 (2006).

Suzuki Y., *In Shape Memory Materials*. Otsuka K., Wayman C.M., (Eds.), Cambridge, 145-147 (1998).

OBȚINEREA UNOR ALIAJE Fe-Mn-Si-Cr-Ni CU MEMORIA FORMEI PRIN TEHNOLOGIA PULBERILOR

(Rezumat)

Cu ajutorul microscopului cu scanare electronică şi difracției de raze X au fost investigate textura precum şi modificările microstructurale ale unor pulberi având compoziția nominală 14Mn-6Si-9Cr-5Ni (%). După sinterizare, probele obținute au fost laminate la cald, la 1370 K, după care a fost realizată din nou difracție de raze X pentru a putea pune în evidență prezența martensitei ε. Probele au fost deformate la cald cu ajutorul unui dispozitiv cilindric pentru a se putea imprima forma caldă în vederea testării efectului de memoria formei prin ciclări termice.

BULETINUL INSTITUTULUI POLITEHNIC DIN IAŞI
Publicat de
Universitatea Tehnică „Gheorghe Asachi” din Iaşi
Tomul LVII (LXI), Fasc. 1, 2011
Secția
ŞTIINȚA ŞI INGINERIA MATERIALELOR

ORTHOSIS „COMARNA” – CALCULATION OF THE SHEAR RIVETS

BY

ADY RANCEA*

*"Gheorghe Asachi" Technical University of Iaşi,
Department of Physical Education and Sports

Received: February 3, 2011
Accepted for publication: March 28, 2011

Abstract. The paper shows the calculation model of the shear rivets of an original orthosis „Comarna” type.

Key words: biomechanics, rivets, orthosis, tendon.

1. Introduction

Orthosis is being used for the recovery of the Achilean tendon after surgical treated injury. „Comarna” orthosis was used for the first time in 2007 by Bogdan Dimitriu for the recovery of a patient from the village with the same name.

It must be said that designing of this type of devices is being done mainly to be light, rigid and to ensure a controlled mobility. These devices are used for the recovering of patients in the hospitals, in the fitness rooms, at the based sports clubs and at by home users.

*Corresponding author; *e-mail*: rancea_ady_2008@yahoo.com

2. Model

So while walking and at rest, patient's weight is taken by rivets, a hinge plate that secures the arm and its axis (Buzdugan *et al.*, 1980; Budescu 2005; Denischi *et al.,* 1989; Drăgulescu *et al.,* 1993). These elements are submitted to shear forces Fig. 1.

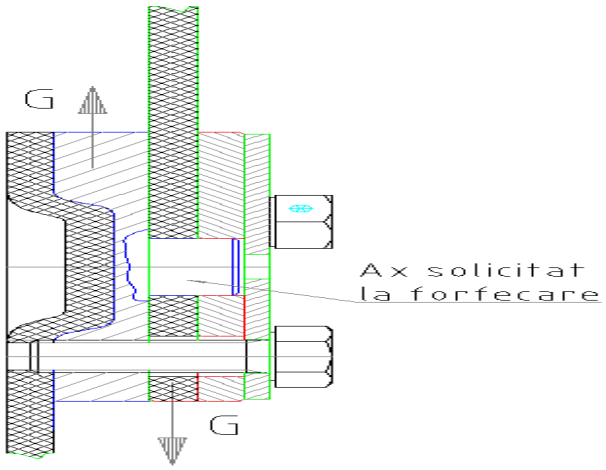

Fig. 1 – Scheme application shear axis (Rancea, 2011).

Shaft diameter is determined from the condition that the shear stresses are lower than allowable shear strength of the material.

$$\tau_f = \frac{G \cdot \psi}{\frac{\pi}{4} \cdot d_{ax}^2} \leq \tau_{af}, \quad [\text{N/mm}^2] \tag{1}$$

where:

ψ = 1.8 is a factor of impact;
τ_{af}= 0,2 $R_{p0,2}$ N/mm^2- allowable shear strength of the material;
d_{ax} = diameter of rotating shaft (mm);
G = static force acting on the shaft, taken as the weight of the patient.

$$d_{ax} = \sqrt{\frac{G \cdot \psi}{\frac{\pi}{4} \cdot \tau_{af}}}, \quad [\text{mm}] \tag{2}$$

2.1. Calculation of the Shear Rivets on Share Stress

Riveted joints are part of the orthosis, and functions as a couple of 5 class type that enables the controlled rotation of angle of the arms (Buzdugan *et al.,* 1980; Budescu 2005; Denischi *et al.,* 1989; Drăgulescu *et al.,* 1993).

The calculus total static shear strength is given by the patient's weight.

Total dynamic shear force is given by:

$$F_{df} = \psi \cdot G, \qquad [\text{N}] \tag{3}$$

The constructive solutions consists in a number of 4 rivets that secure the hinge plate subsequently the share force by rivet becomes:

$$T=F_{df} / 4, \qquad [\text{N}] \tag{4}$$

Shear stress of the rivet must be less than the allowable shear tension.

$$\tau = \frac{T}{A} \leq \tau_{af}, \qquad [\text{N}] \tag{5}$$

$$A = \frac{\pi \cdot d^2_{riv}}{4}, \qquad [\text{mm}^2] \tag{6}$$

where:

A is the sectional area mm^2 rivet;

$\tau_{af} = 22\ \text{N/mm}^2$ - voltage is allowable shear for aluminum;

d_{riv} = rivet diameter is mm.

Rivet diameter is given by:

$$d_{riv} \geq \sqrt{\frac{4 \cdot T}{\pi \cdot \tau_{af}}}, \qquad [\text{mm}] \tag{7}$$

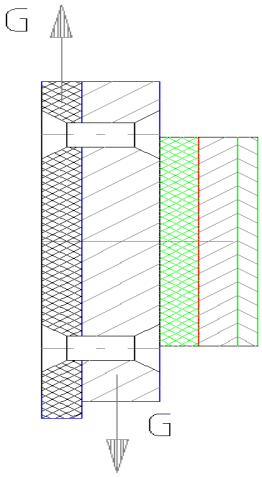

Fig. 2 – Scheme application shear rivets.

Orthosis „Comarna" resulting from the design and implementation is shown in Fig. 3.

a

b

c

Fig. 3 – Images Comarna orthosis: *a* – right side view; *b* – left lateral view; *c* – front view.

3. Conclusions

The standard SR EN 13291:2007 (EN 132921:2007) „Individual protection equipment. Ergonomic principles" is a guide related to the ergonomic characteristics of such products. Among the things that must be taken in consideration we are mentioning:

– „Comarna" orthosis ensures the protection against specified risks and is from an ergonomically point of view proper for the provided utilization;

– „Comarna" orthosis allows making specifically movements

– „Comarna" orhosis achieves adaptability and maintaining on the body: adjustment, stability of adjustments

– „Comarna" orthosis doesn't causes rashes and discomfort;

– the orthosis doesn't make worst the biomechanically characteristics: weight distribution, inertial forces distribution on the human body, limitation or stopping movements, abrasion or compression on teguments and muscles, raising of vibration;

– the orthosis isn't a stress factor for the patient.

REFERENCES

Budescu E., Iacob I., *Bazele biomecanicii în sport*. Ed. Univ. „Alexandru Ioan Cuza", Iaşi, 2005.

Buzdugan Gh., *Rezistenţa materialelor*. Ed. Tehn., Bucureşti, 1980.

Denischi A., Marin, I.G., Antonescu, D., Petrescu, L., *Biomecanica*. Ed. Academiei, Bucureşti, 1989.

Drăgulescu D., Toth Taşcău M., *Elemente de inginerie mecanică*. **I-II**, Ed. Univ. Tehn. Timişoara, 1993.

Rancea A., *Orteza „Comarna" pentru recupararea traumei pe tendonul lui Ahile post traumatic*. Ed. Univ. Tehn. „Gh. Asachi" Iaşi, Referat, *3,* Teză de doctorat, 2011.

ORTEZA „COMARNA"- CALCULUL DE DIMENSIONARE LA FORFECARE

(Rezumat)

Lucrarea prezintă modelul de calcul al niturilor la solicitarea de forfecare a unei orteze originale tip „Comarna".